SoftCOM '18
tutorials

# Matrix Pencil Method applied to electromagnetics, smart metering and bioelectromagnetics phenomena

by

**Khalil El Khamlichi Drissi**

**Clermont Auvergne University, France**

**September 13 - 15, 2018.**

Tutorial SoftCOM 2018

**Pr. Khalil EL KHAMLICHI DRISSI**

# Matrix Pencil Method applied to electromagnetics, smart metering and bio electromagnetics phenomena

# Identity of the Laboratory

- Employees:
  - 198 Faculty members and researchers;
  - 27 Engineers, Technicians and Administrative;
  - 151 PhD students, postdocs or CSD.

- Budget:
  - The annual research budget is approximately 6.3 M€ of which 93% came from own resources (European projects, ANR, PIA, CPER, FUI, BPI contracts, Industrial, ...). Adding salaries, it amounts to almost 16 M€.

- Research achievements for last 5 years:
  - 2400 publications and 32 patents;
  - 19 European projects;
  - 58 national projects;
  - 60 industrial projects.

# Structure of the Laboratory

INSTITUT PASCAL
sciences de l'ingénierie et des systèmes

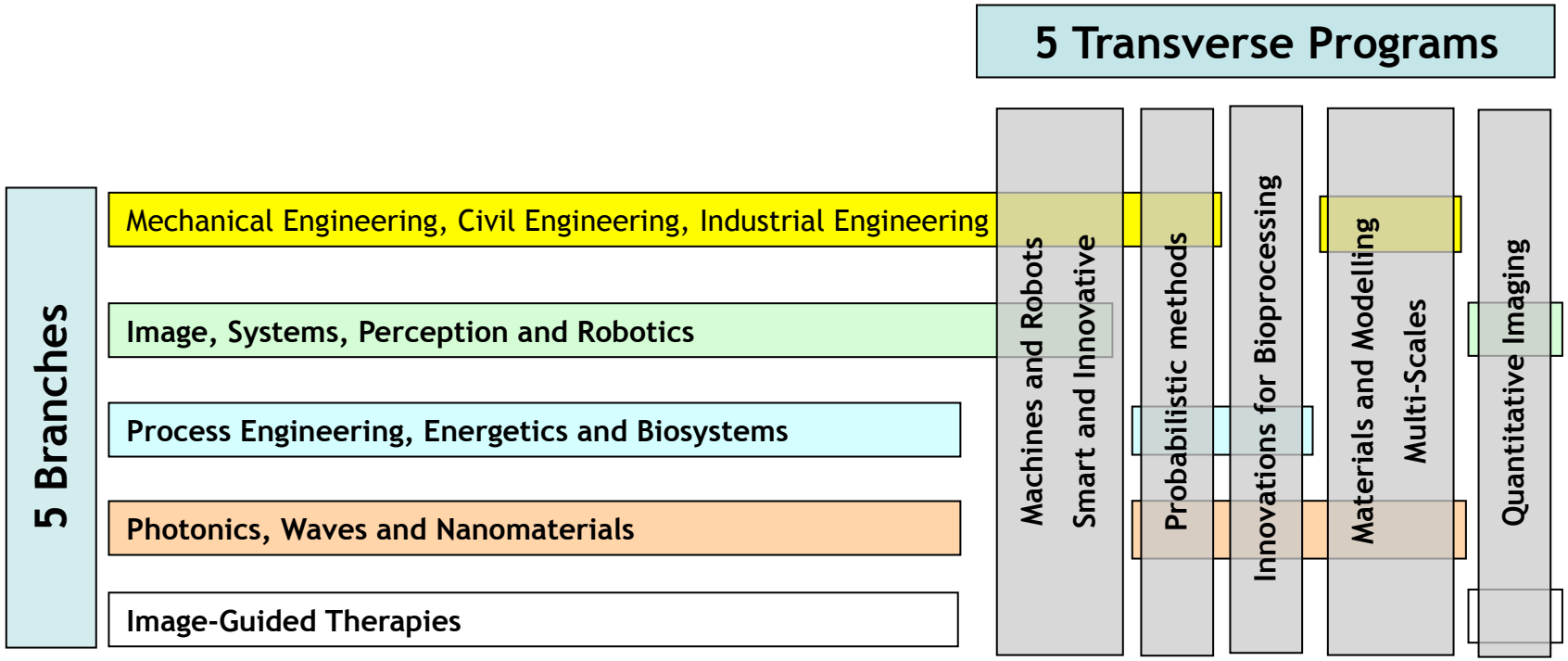

# Structure of the Laboratory

5 branches (Scientific heart):

- Mechanical Engineering, Civil Engineering, Industrial Engineering (M3G)
  65 academic staff (61 EC, 4 BIATSS)

- Image, Systems, Perception and Robotics (ISPR)
  31 academic staff (24 EC, 2 C, 5 BIATSS)

- Process Engineering, Energetics and Bio systems (GePEB)
  27 academic staff (23 EC, 1 PR Emeritus, 3 BIATSS)

- **Photonics, Waves and Nano materials (PHOTON)**
  **41 academic staff (30 EC, 1 C, 3 Emeritus PR, 7 BIATSS)**

- Image-Guided Therapy (TGI)
  61 academic staff (50 EC, 3C, 8 BIATSS)

# ElectroMagnetique Compatibility Group (EMC)

**3 Professors - 4 Associate Professors**
**1 Associate Researcher - 1 Engineer - 5 PhD - 1 PostDoc**

- Area of interest: development of numerical models for electromagnetic characterization. It is applied to complex systems, scenes and wave / structure interaction.

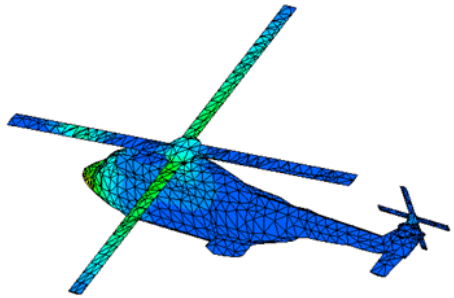

- Objectives:
  - Evaluation of electromagnetic couplings
  - Development of experimental methods for the generation of disruptive electromagnetic environment or noise reduction
  - Analysis of information transmission and communication
  - Electronic Systems Immunity

# Theoretical background: Matrix Pencil Method

- MPM algorithm in space domain per example
- Finite series of exponential model with damped factor $\alpha_i$

$$y(z) = x(z) + n(z) = \sum_{i=1}^{M} R_i e^{S_i z} + n(z) \; ; \; 0 \le z \le L$$

$$R_i = a_i + jb_i$$

$$S_i = \alpha_i + j\beta_i$$

$$y(kZ_e) = x(kZ_e) + n(kZ_e) \approx \sum_{i=1}^{M} \mathcal{R}_i q_i^k + n(kZ_e)$$

$$Z_e = \Delta z \quad and \quad q_i = e^{s_i Z_e} \quad where \quad s_i = \alpha_i + j\beta_i$$

- Hankel matrix of N samples (structured matrix)

$$\mathbf{Y} = \begin{bmatrix} y(1) & y(2) & \cdots & y(L) & y(L+1) \\ y(2) & y(3) & \cdots & y(L+1) & y(L+2) \\ \vdots & \vdots & \cdots & \vdots & \vdots \\ y(N-L) & y(N-L+1) & \cdots & y(N-1) & y(N) \end{bmatrix}_{(N-L)\times(L+1)}$$

$\mathbf{Y}_1$ $\mathbf{Y}_2$

# Matrix Pencil Method to estimate a function

- Matrix decomposition

$$\mathbf{Y}_1 = \mathbf{Z}_1 \cdot \mathbf{R} \cdot \mathbf{Z}_2; \qquad \mathbf{Y}_2 = \mathbf{Z}_1 \cdot \mathbf{R} \cdot \mathbf{Z}_0 \cdot \mathbf{Z}_2$$

- Van der Monde Matrices

$$\mathbf{Z}_1 = \begin{bmatrix} 1 & 1 & \cdots & 1 \\ z_1 & z_2 & \cdots & z_M \\ \vdots & \vdots & \cdots & \vdots \\ z_1^{N-L-1} & z_2^{N-L-1} & \cdots & z_M^{N-L-1} \end{bmatrix}_{(N-L)\times M} \qquad \mathbf{Z}_2 = \begin{bmatrix} 1 & z_1 & \cdots & z_1^{L-1} \\ 1 & z_2 & \cdots & z_2^{L-1} \\ \vdots & \vdots & \cdots & \vdots \\ 1 & z_M & \cdots & z_M^{L-1} \end{bmatrix}_{M\times L}$$

$$\mathbf{Z}_0 = \mathrm{diag}\left[z_1, z_2, \cdots, z_M\right]; \qquad \mathbf{R} = \mathrm{diag}\left[\mathcal{R}_1, \mathcal{R}_2, \cdots, \mathcal{R}_M\right]$$

- We construct eigenvalues problem

$$\det\left\{\mathbf{Y}_2 - \lambda \mathbf{Y}_1\right\} = 0 \qquad \text{or} \qquad \det\left\{\mathbf{Z}_1 \mathbf{R}\left[\mathbf{Z}_0 - \lambda \mathbf{I}_M\right]\mathbf{Z}_2\right\} = 0$$

# Singular Value Decomposition (SVD)

- Any Matrix Y can be decomposed on singular values:

$$\mathbf{Y} = \mathbf{U}\Sigma\mathbf{V}^T \qquad \begin{aligned}\mathbf{U}\mathbf{U}^T &= \mathbf{I}\\ \mathbf{V}\mathbf{V}^T &= \mathbf{I}\end{aligned}$$

- Application to left and right Hankel matrices

$$\begin{aligned}\mathbf{Y}_1 &= \mathbf{U}\Sigma\mathbf{V}_1^T\\ \mathbf{Y}_2 &= \mathbf{U}\Sigma\mathbf{V}_2^T\end{aligned}$$

$$\Sigma = diag\left\{\sigma_1, \sigma_2, \cdots, \sigma_h\right\}, \text{with} h = \min\left\{N-L, L+1\right\}$$

$$\sigma_1 \geq \sigma_2 \geq \cdots \geq \sigma_M \geq \sigma_{M+1} \geq \cdots \geq \sigma_h$$

- M is the number of significant singular values
- We construct a filtered matrices

$$\begin{aligned}\mathbf{U}^M &= \mathbf{U}\left(1:N-L, 1:M\right)\\ \mathbf{V}_1^M &= \mathbf{V}_1\left(1:L, 1:M\right)\\ \mathbf{V}_2^M &= \mathbf{V}_2\left(2:L+1, 1:M\right)\\ \Sigma^M &= \Sigma\left(1:M, 1:M\right)\end{aligned}$$

# Function signatures (Poles and Residues)

- We extract $\left\{ z_i \right\}_{1 \le i \le M}$ eigenvalues problem with smaller size matrix,

$$\det\left\{ \mathbf{V}_2^{\mathbf{M}} - \lambda \mathbf{V}_1^{\mathbf{M}} \right\} = \mathbf{0}$$

- Residues $\mathcal{R}$ are derived by solving a Van Der Monde linear system,

$$\begin{bmatrix} y(1) \\ y(2) \\ \vdots \\ y(N) \end{bmatrix} = \begin{bmatrix} 1 & 1 & \cdots & 1 \\ z_1 & z_2 & \cdots & z_M \\ \vdots & \vdots & \cdots & \vdots \\ z_1^{N-1} & z_2^{N-1} & \cdots & z_M^{N-1} \end{bmatrix} \cdot \begin{bmatrix} \mathcal{R}_1 \\ \mathcal{R}_2 \\ \vdots \\ \mathcal{R}_M \end{bmatrix}$$

# High resolution parametric methods

**Matrix Pencil: a complex exponential basis with mitigation consideration of a white Gaussian noise (measurement scenario)**

Noise variance *n(t)* $\sigma = 0.1$

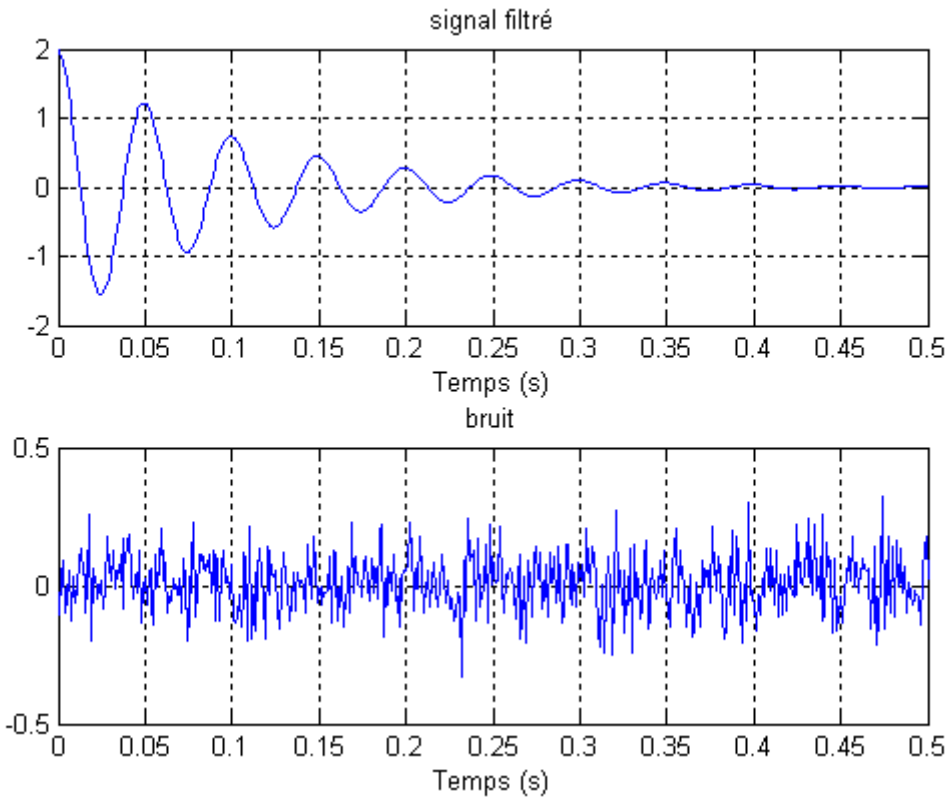


Reconstructed Signal

$$x(t) = 2\cos(40\pi t)e^{-10t} + n(t)$$

$$s_{1,2} = -10 \pm 40\pi j$$

$$\Re_{1,2} = 1 \mp 0j$$

# High resolution parametric methods

**Choosing of window size, position and the number of samples**

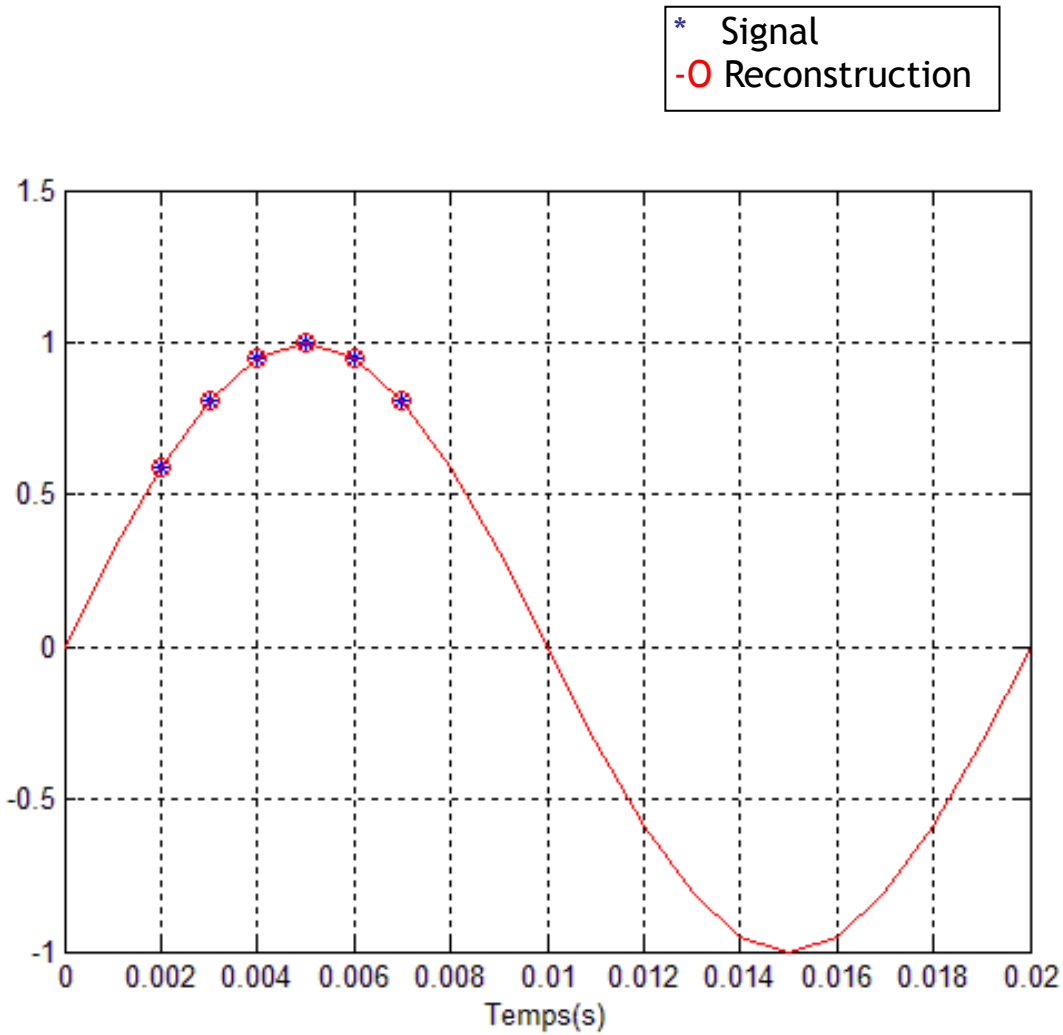


$$x(t) = \sin(2\pi 50 t)$$

**Signature**

$$s_{1,2} = 0 \pm 2\pi 50 j$$
$$\Re_{1,2} = 0 \pm 0.5 j$$

$$s_{1,2} = 0 \pm 2\pi 50 j$$
$$\Re_{1,2} = 0 \pm 0.5 j$$

$$s_{1,2} = 0 \pm 2\pi 50 j$$
$$\Re_{1,2} = 0 \pm 0.5 j$$

# High resolution parametric methods

**Application to the case of the first Hankel function $H_0$:**
**Three basic functions (M=3)**

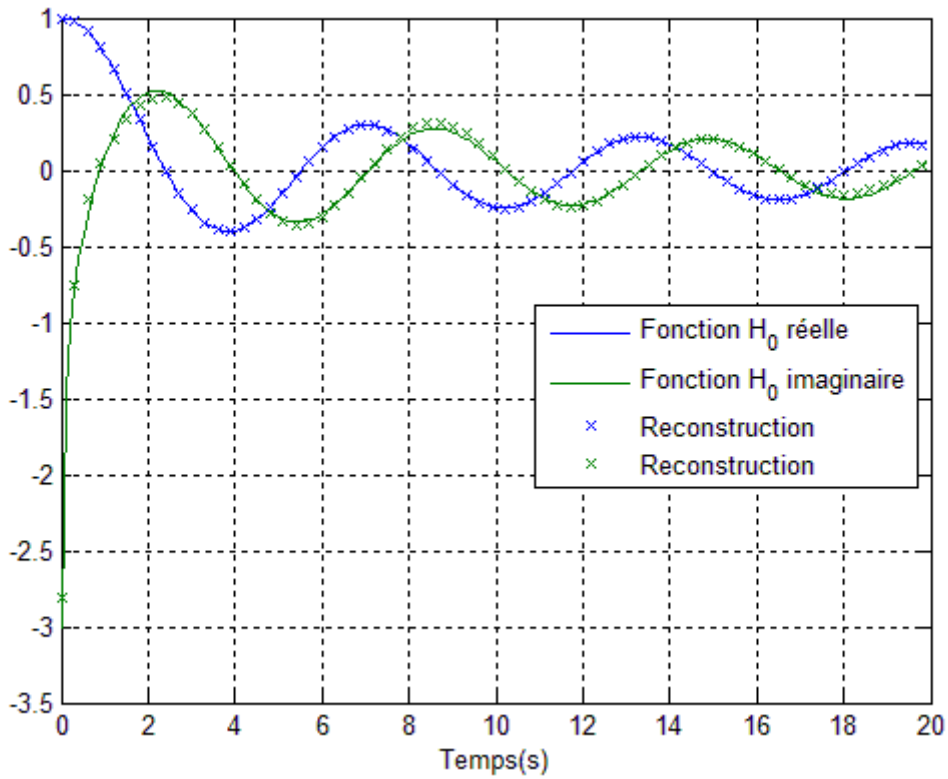


**Signature**

$$s_1 = -6.5817 + 1.6111i$$
$$s_2 = -0.0410 + 1.0015i$$
$$s_3 = -0.6509 + 1.0516i$$
$$\Re_1 = 0.2846 - 1.5600i$$
$$\Re_2 = 0.2678 - 0.2797i$$
$$\Re_3 = 0.4189 - 0.6490i$$

# Radiation from thin wire systems

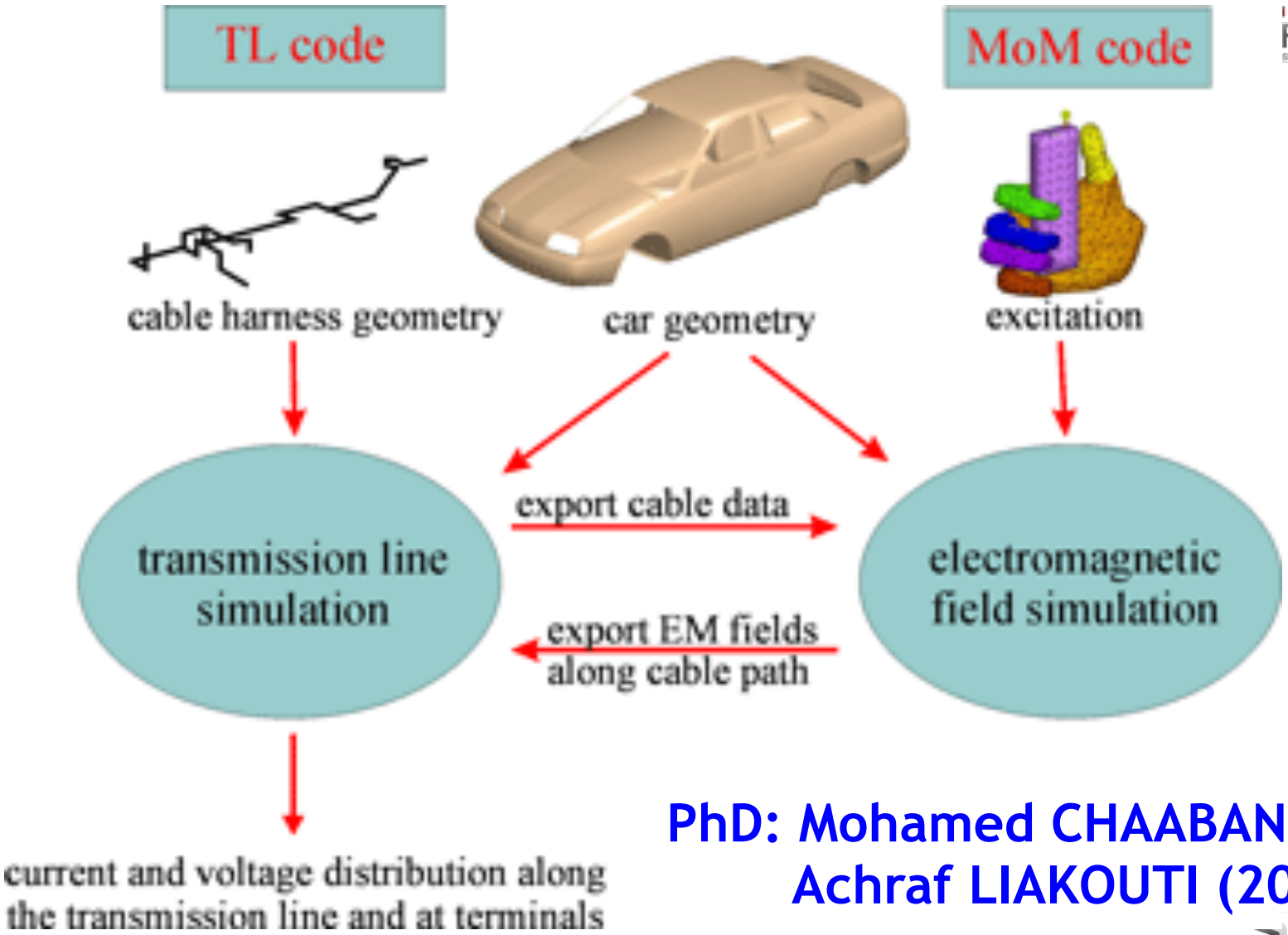


**PhD: Mohamed CHAABAN (2011)**
**Achraf LIAKOUTI (2017)**

# Current distribution

Obtaining the current distribution over the wire systems by:

- **Measurement:** Difficulty to access especially in case of embedded wires (wall, ground).
- **Transmission lines theory:** Analytical model,
- **Antenna theory:** Non linear resolution.

# Theoretical model to evaluate radiated field

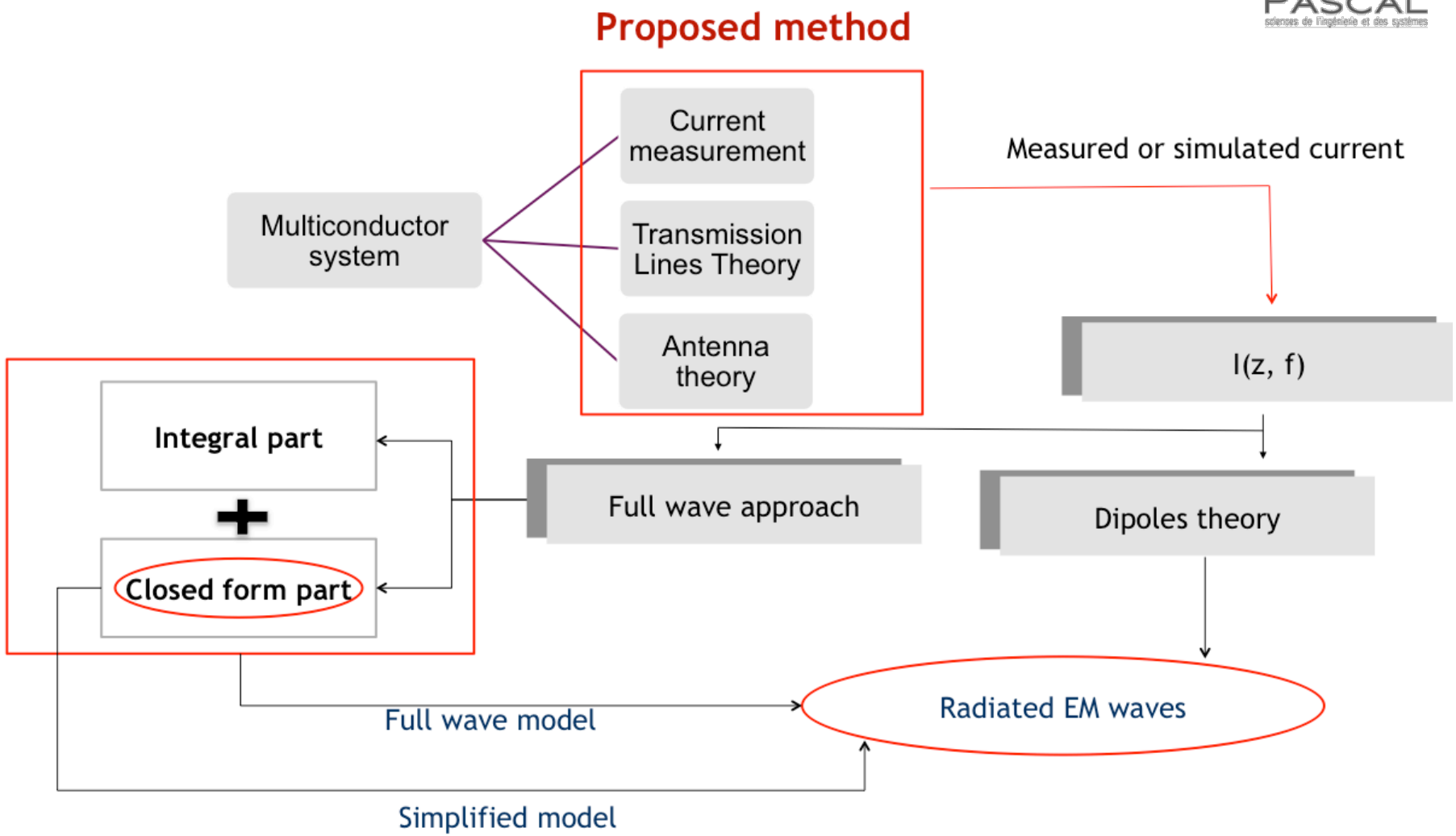

# Radiation from thin wire systems

## Vector Potential and Green Function

$$\vec{A} = \frac{\mu}{4\pi}\int I(Z)\,G(Z)\,dZ\,\vec{e_z}$$

Green function for homogeneous media

$$G(Z) = \frac{e^{-\gamma_0 R(Z)}}{R(Z)}$$

Current distribution → Mathematical Model → EM radiated field

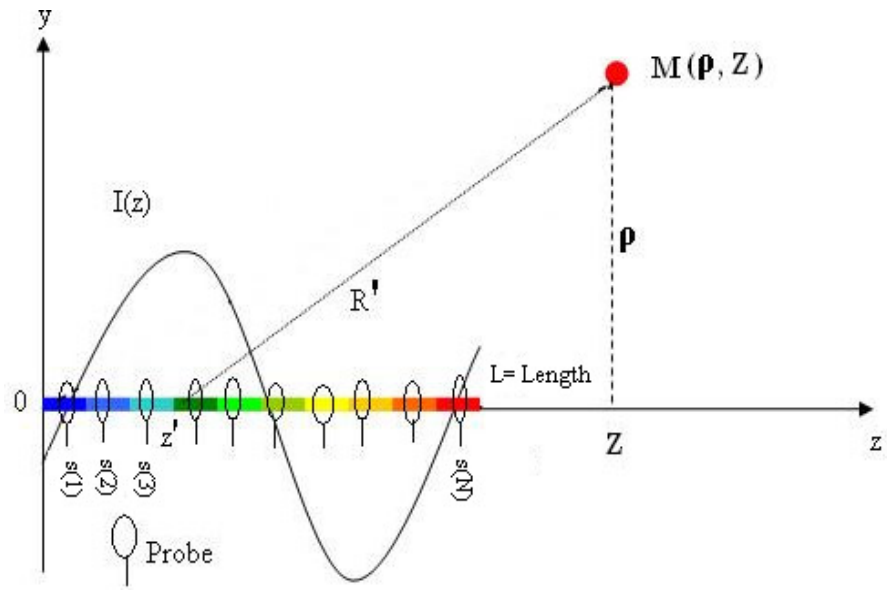

# Radiation from thin wire systems

## Example of a single dipole or a travelling wave antenna (length L)

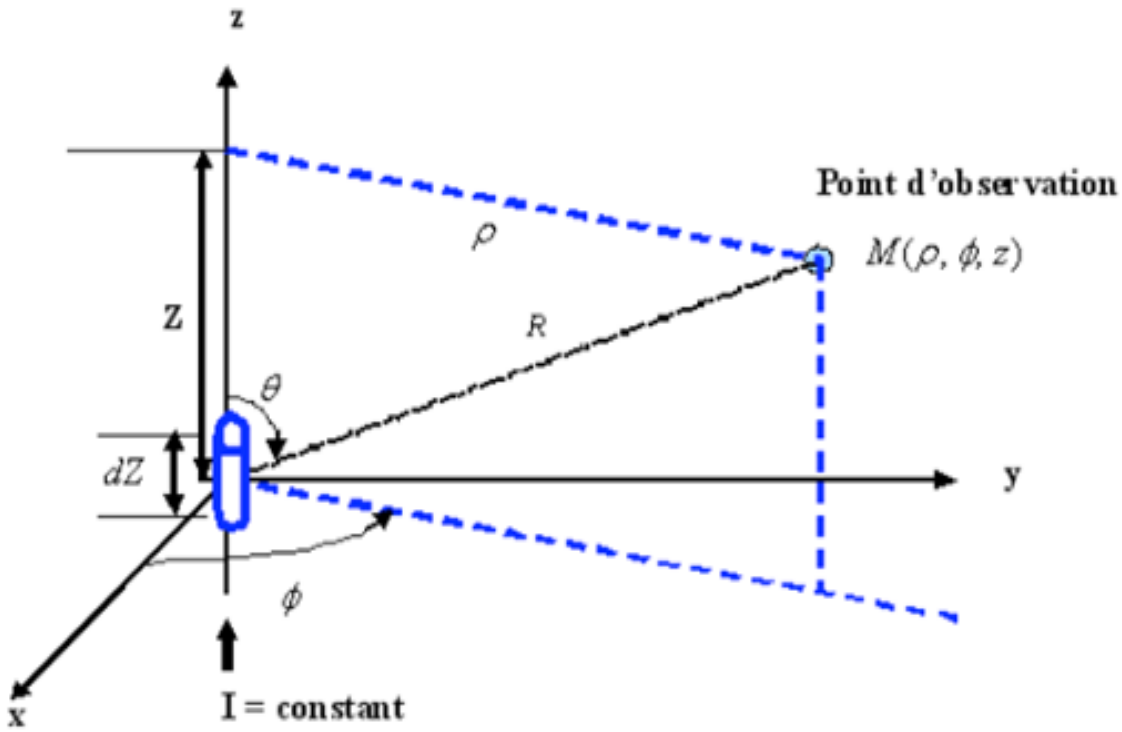


## Cylindrical coordinates

# EM field in cylindrical coordinates

## Evaluation of Electromagnetic Fields

$$\overrightarrow{H} = H\varphi\, \vec{e}\varphi$$

$$\vec{E} = E\rho\vec{e}\rho + Ez\vec{e}z$$

Avec : $$H\varphi = -\frac{1}{\mu}\frac{dAz}{d\rho}$$

$$E\rho = \frac{s}{\gamma^2}\frac{d^2Az}{d\rho dZ}$$

$$Ez = \frac{s}{\gamma^2}\left(\frac{d^2Az}{dZ^2} - \gamma^2 Az\right)$$

# EM field in cylindrical coordinates

$$G_0 = \frac{e^{-\gamma R_0}}{R_0}$$

$$\vec{H}_\phi = \frac{-1}{4\pi\rho\gamma}\left\{\int_{-\frac{L}{2}}^{\frac{L}{2}}\left(I'' - \gamma^2 I\right)e^{-\gamma R_0}dZ_0 + \left[\left(I\gamma\cos\theta_0 - I'\right)e^{-\gamma R_0}\right]_{-\frac{L}{2}}^{\frac{L}{2}}\right\}\vec{e}_\phi$$

$$\vec{E}_\rho = \frac{\eta}{4\pi\rho\gamma^2}\left\{\int_{-\frac{L}{2}}^{\frac{L}{2}}\left(I'' - \gamma^2 I\right)' e^{-\gamma R_0}dZ_0 + \left[\left(\gamma I'\cos\theta_0 - I'' + I\gamma^2\sin^2\theta_0 + I\frac{\gamma}{R_0}\sin^2\theta_0\right)e^{-\gamma R_0}\right]_{-\frac{L}{2}}^{\frac{L}{2}}\right\}\vec{e}_\rho$$

$$\vec{E}_z = \frac{\eta}{4\pi\gamma}\left(\int_{-\frac{L}{2}}^{\frac{L}{2}}\left(I'' - \gamma^2 I\right)G_0 dZ_0 - \left[I\cos\theta_0 G_0' + I' G_0\right]_{-\frac{L}{2}}^{\frac{L}{2}}\right)\vec{e}_z$$

integral parts

closed form part

Under the conditions of transmission line theory, the integral terms vanishes

# Radiation from thin wire systems

## In the case of neglecting integral part

$$\overrightarrow{H_\Phi} = \frac{1}{4\pi\rho}\left[e^{-\gamma R_0}\left(I\cos\theta_0 - \frac{I'}{\gamma}\right)\right]_0^L \overrightarrow{e_\Phi}$$

$$\overrightarrow{E_\rho} = \frac{\eta_0}{4\pi\rho}\left[\frac{e^{-\gamma R_0}}{\gamma R_0}\left(I\sin^2\theta_0 - \gamma R_0\cos\theta_0\left(I\cos\theta_0 - \frac{I'}{\gamma}\right)\right)\right]_0^L \overrightarrow{e_\rho}$$

$$\overrightarrow{E_z} = \frac{\eta_0\gamma}{4\pi}\left[\frac{e^{-\gamma R_0}}{\gamma R_0}\left(\left(1+\frac{1}{\gamma R_0}\right)I\cos\theta_0 - \frac{I'}{\gamma}\right)\right]_0^L \overrightarrow{e_z}$$

# Vertical antenna with voltage source at near end

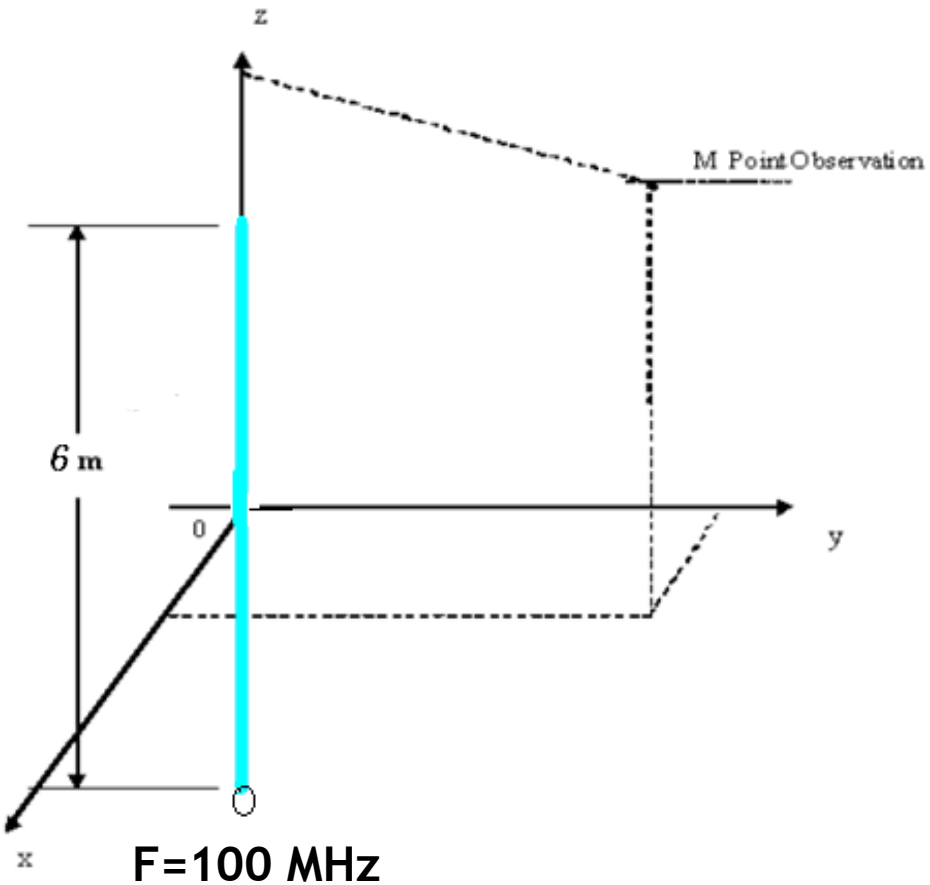


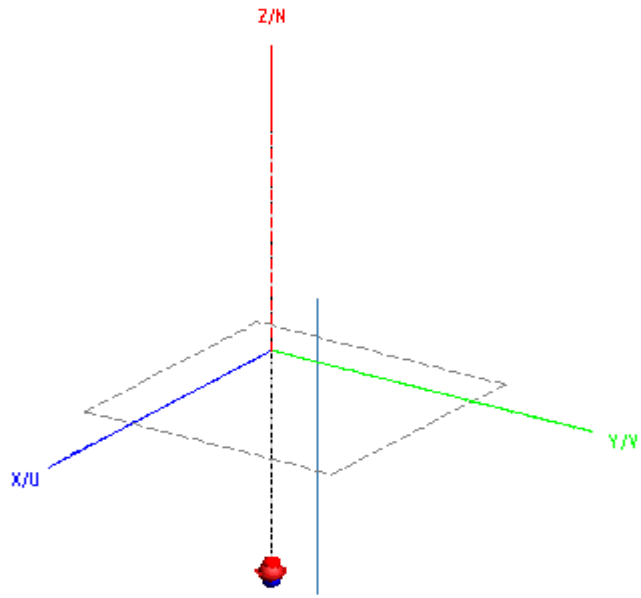


**F=100 MHz**
**V=1 V**

# Reconstruction of current distribution

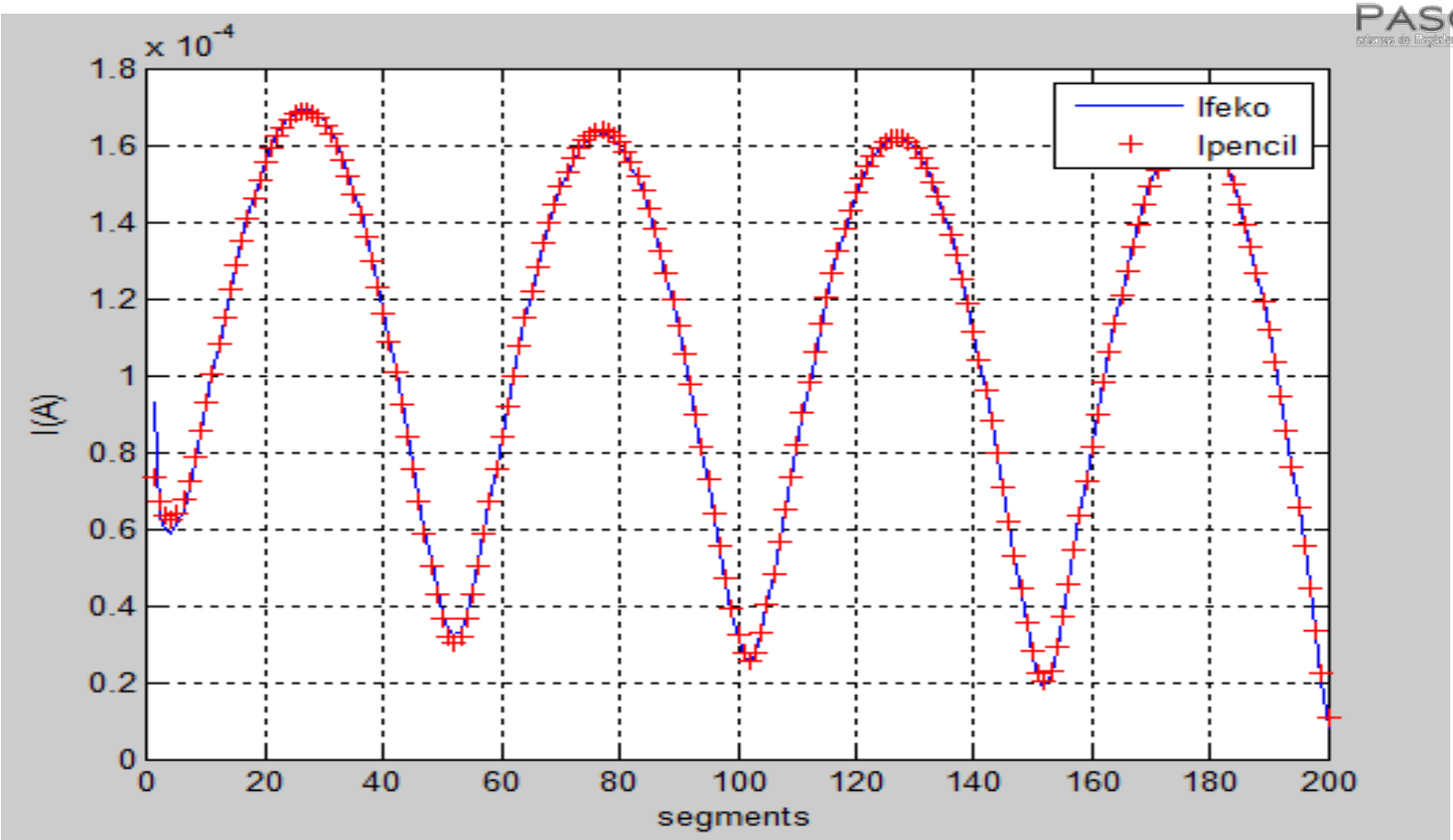


**Excellent agreement between Feko results and results reconstructed by MPM method**

# Total and partial Electrical Field

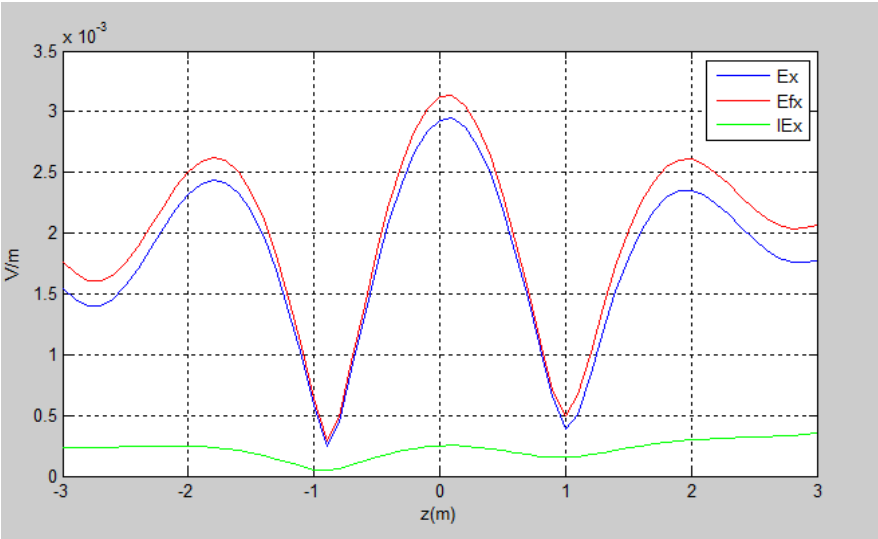


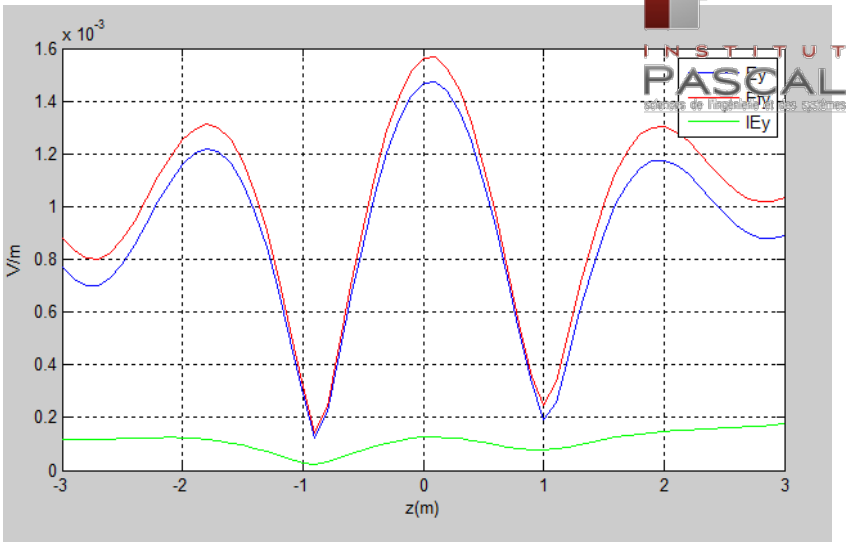


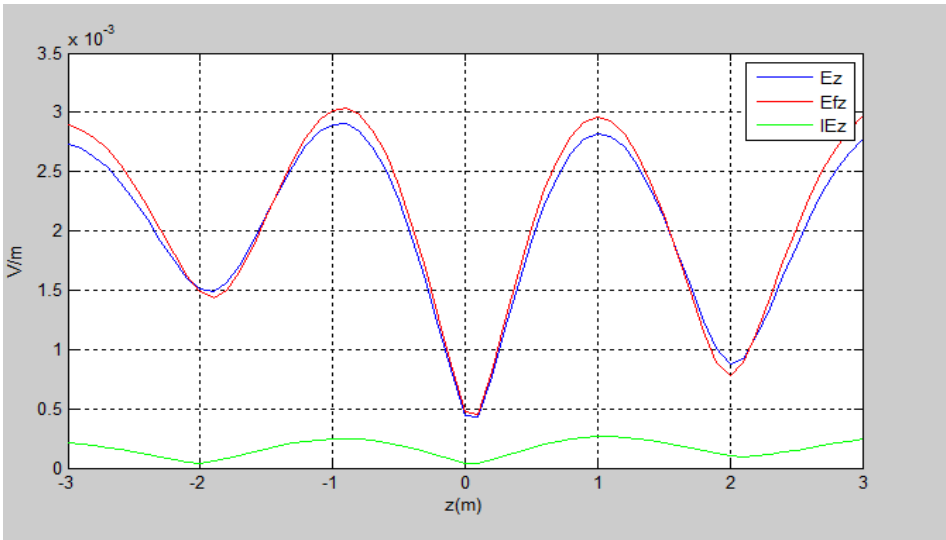


**The integral part can be neglected**

# Total and partial Magnetic Field

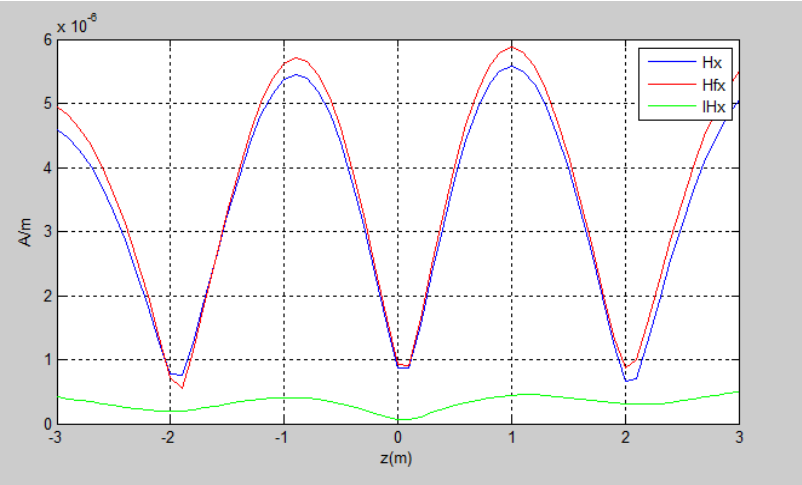


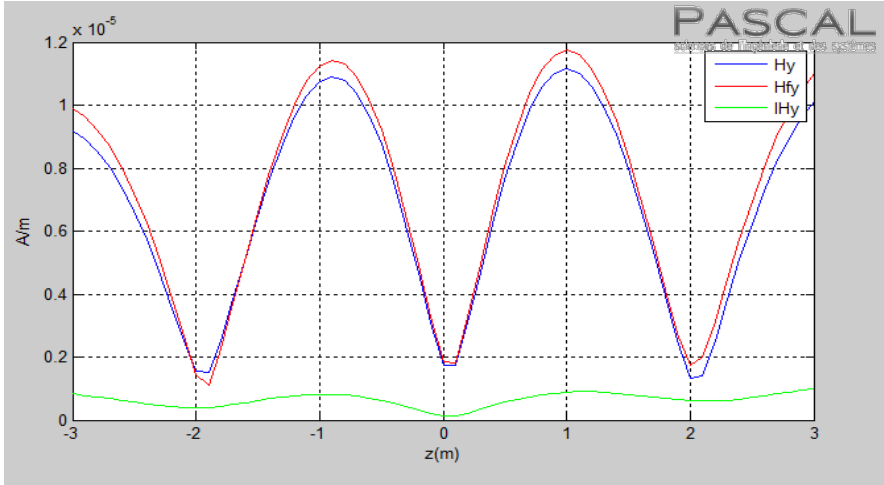


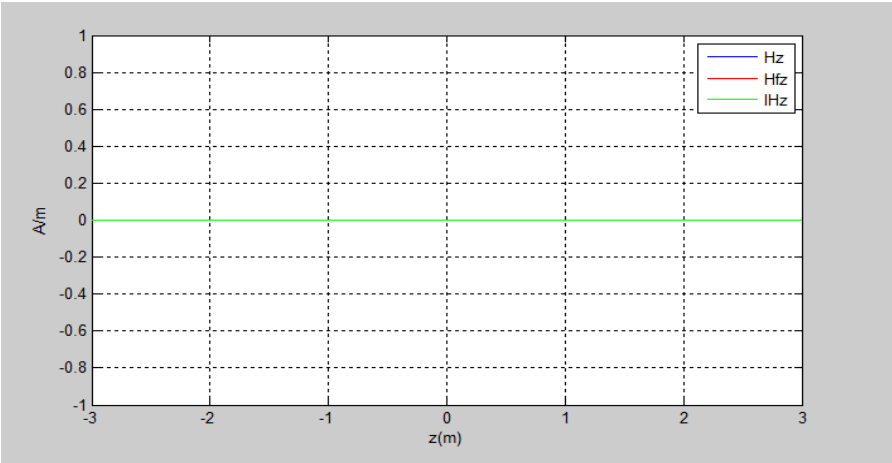


**The integral part can be neglected**

# Vertical antenna with voltage source in the center

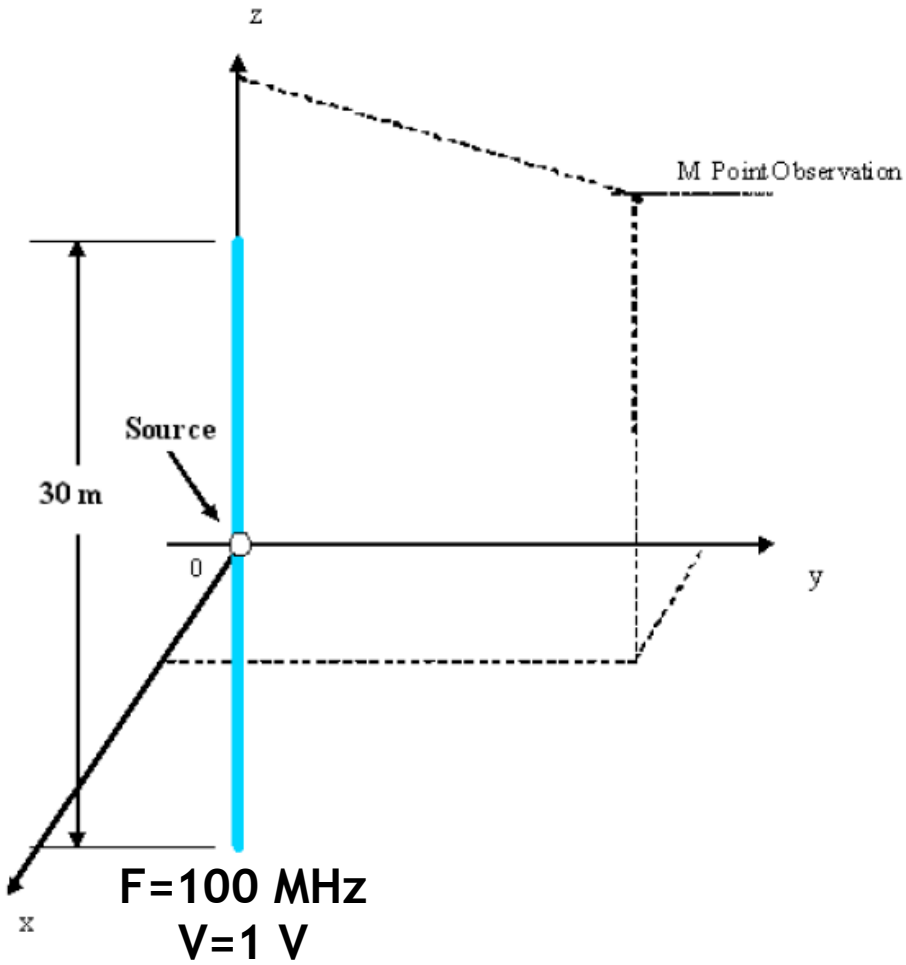


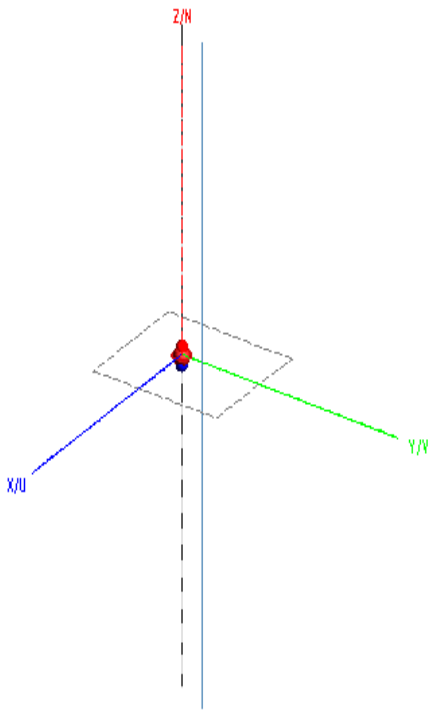

# Reconstruction of current distribution

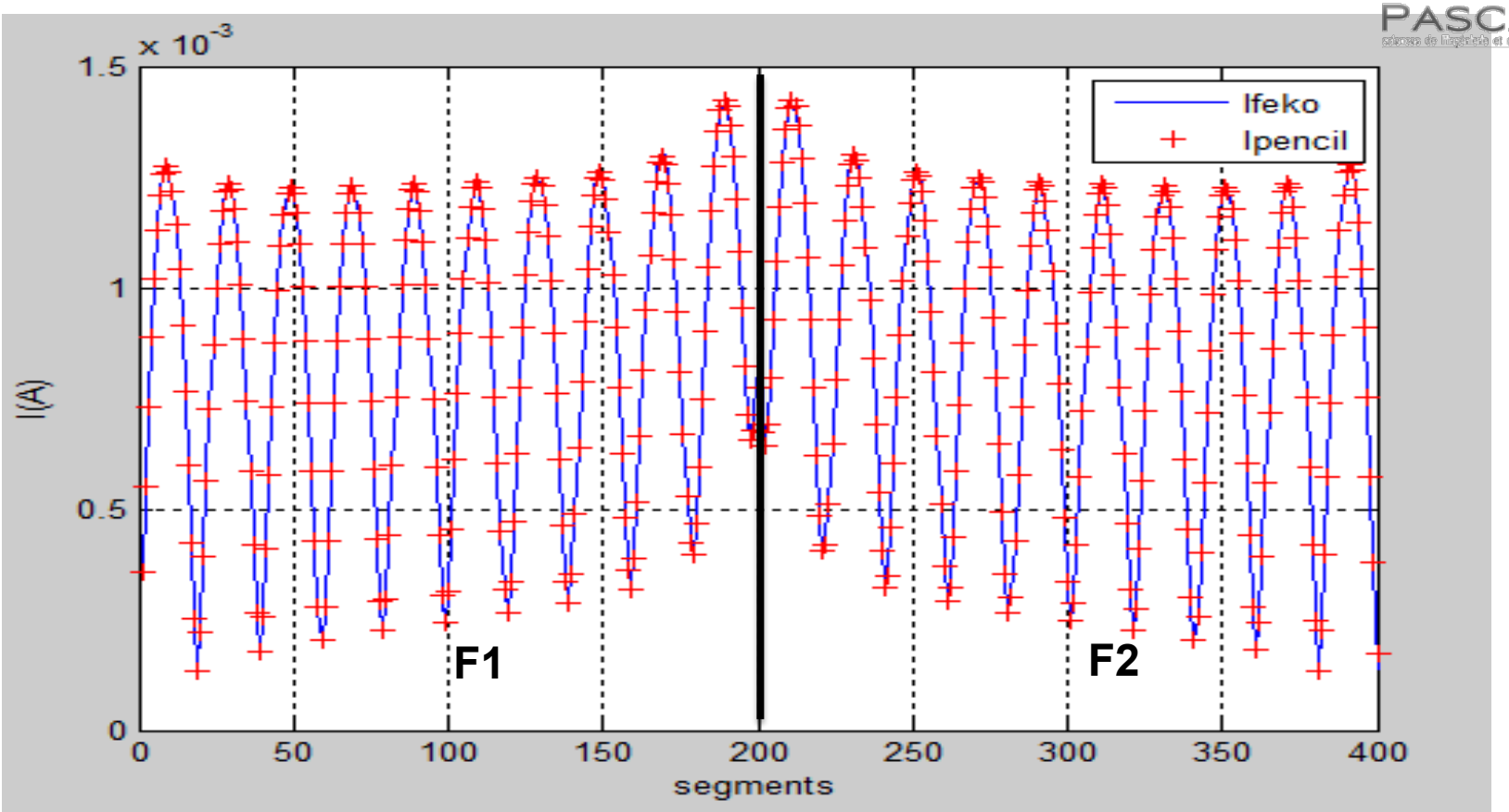


**Excellent agreement between Feko results and results reconstructed by MPM method for each branch F**

# Total and partial Electrical Field

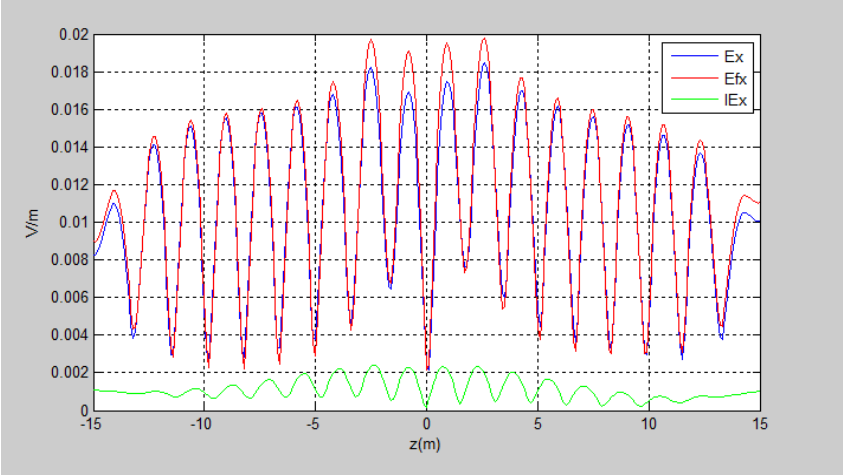


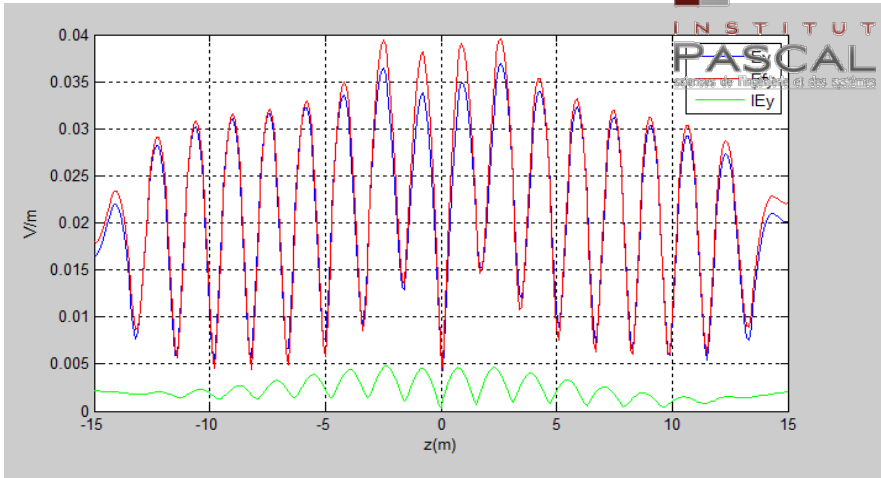


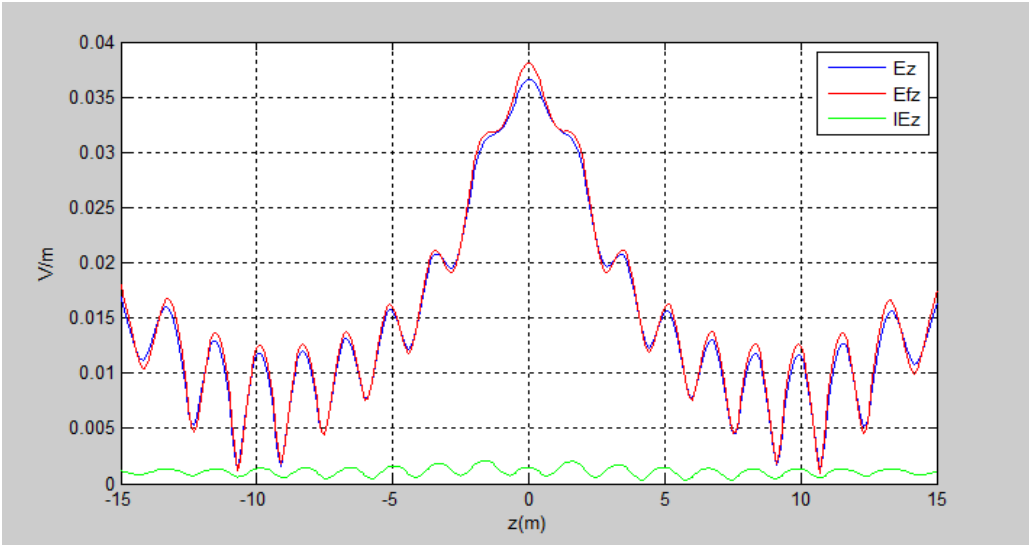


**The integral part can be neglected**

# Total and partial Magnetic Field

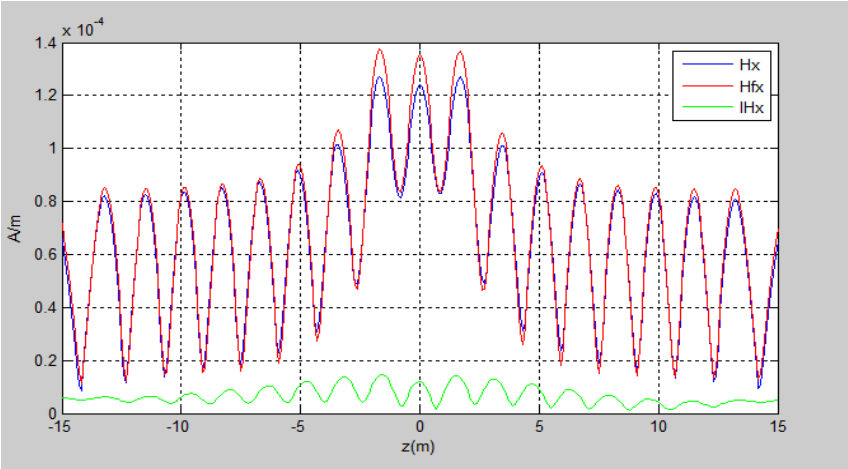


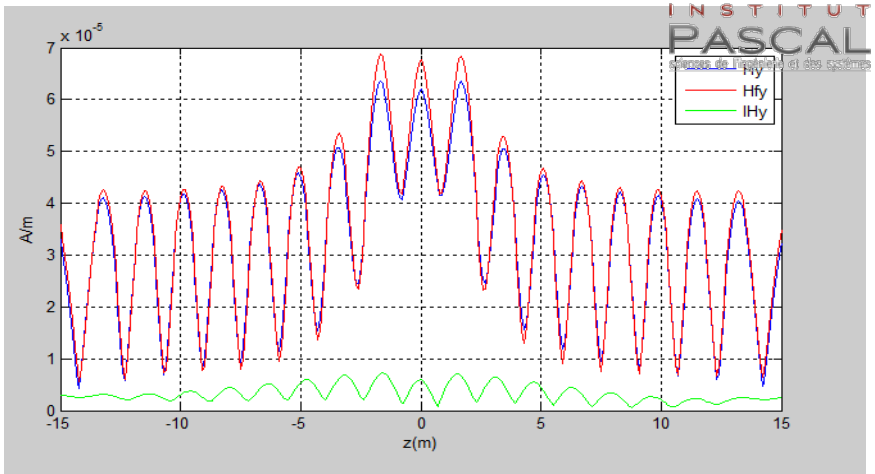


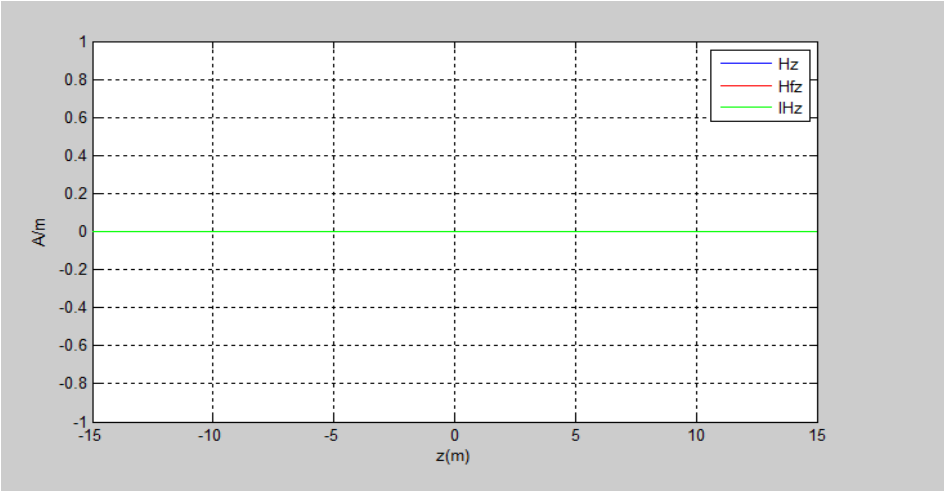


**The integral part can be neglected**

# Feko simulation results

## ❑ Magnetic Field

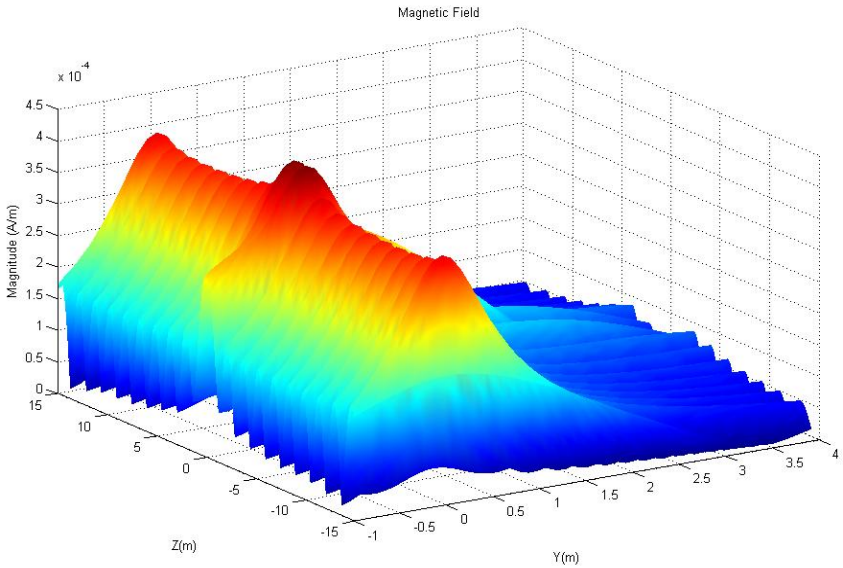


## ❑ Electric Field

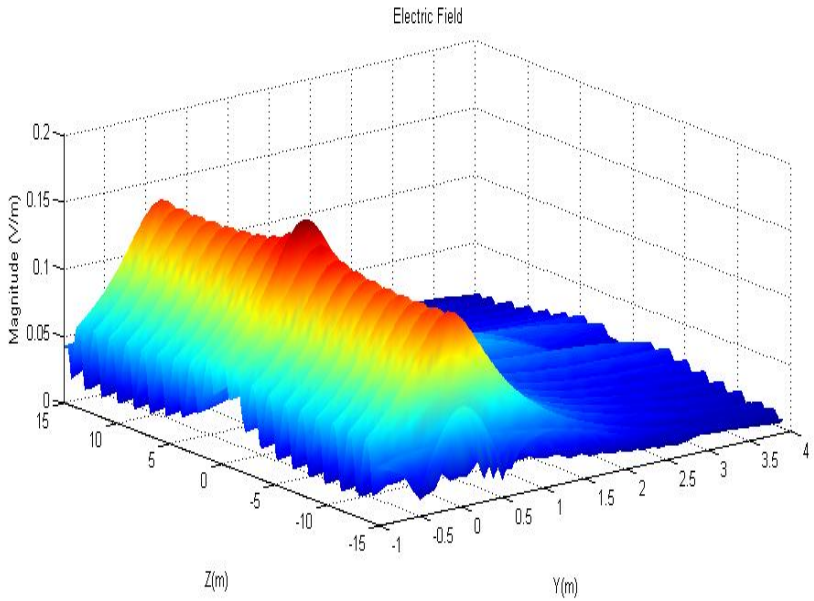

# Simulation results (Feko and our approach)

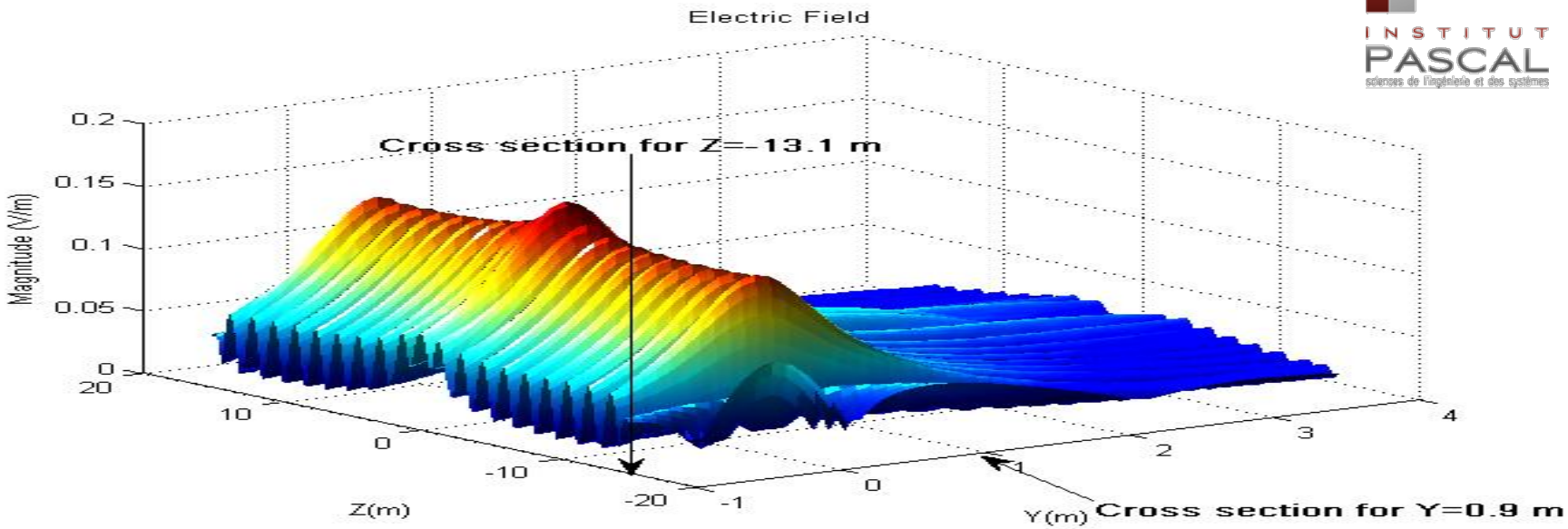


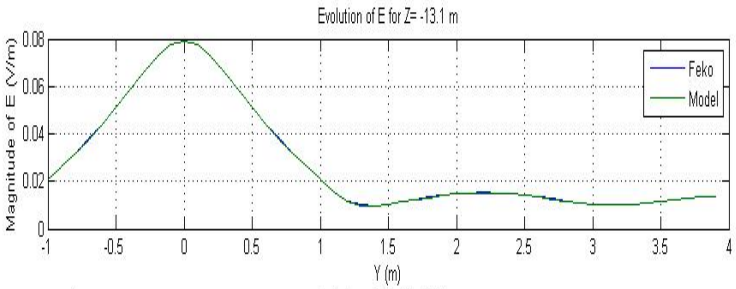


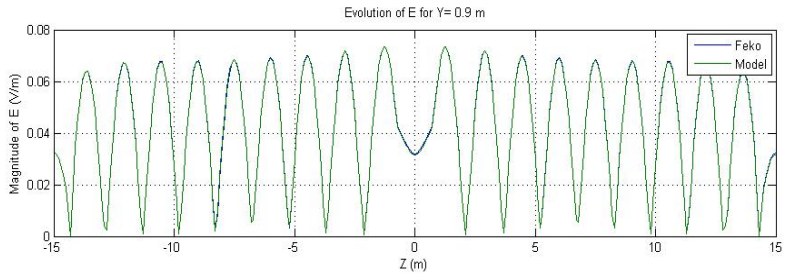


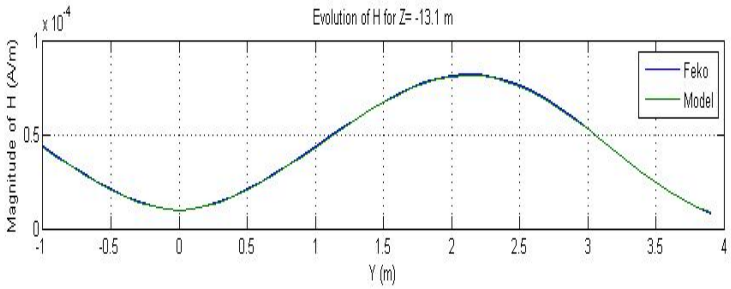


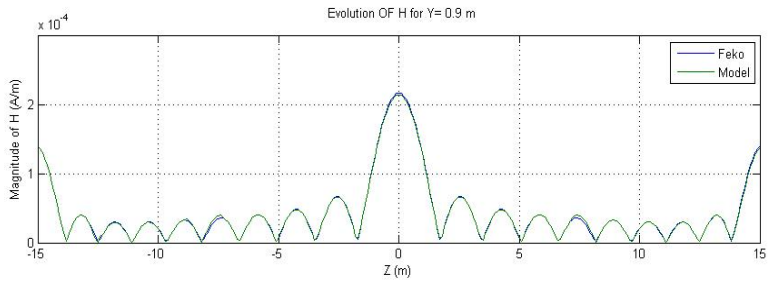

# L-shaped antenna with voltage source and resistive load

F=100 MHz
V=1 V
R=5 Ω

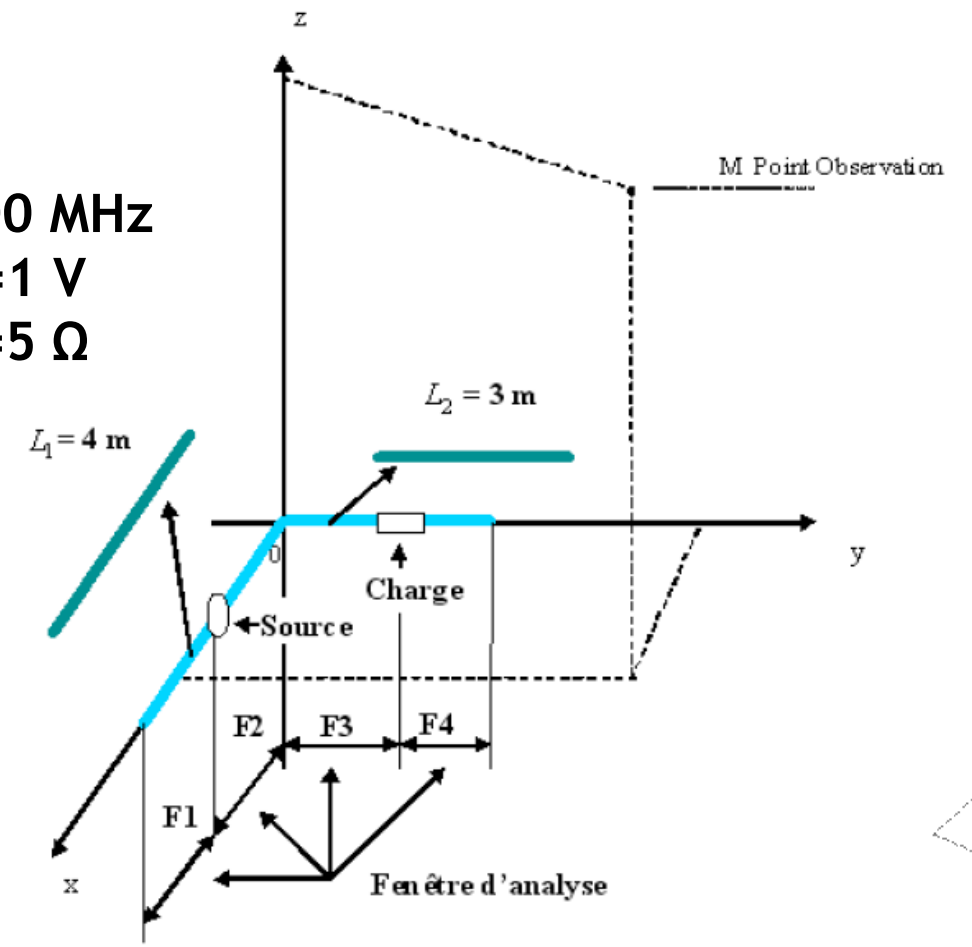


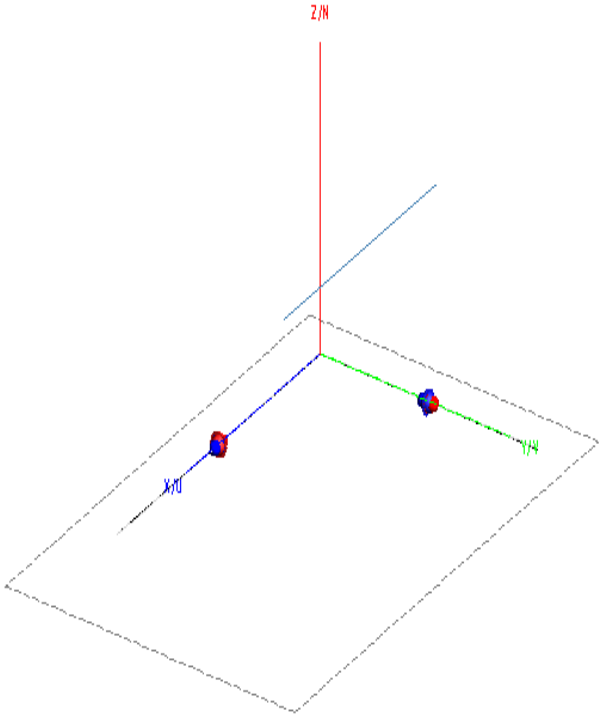

# Reconstruction of current distribution

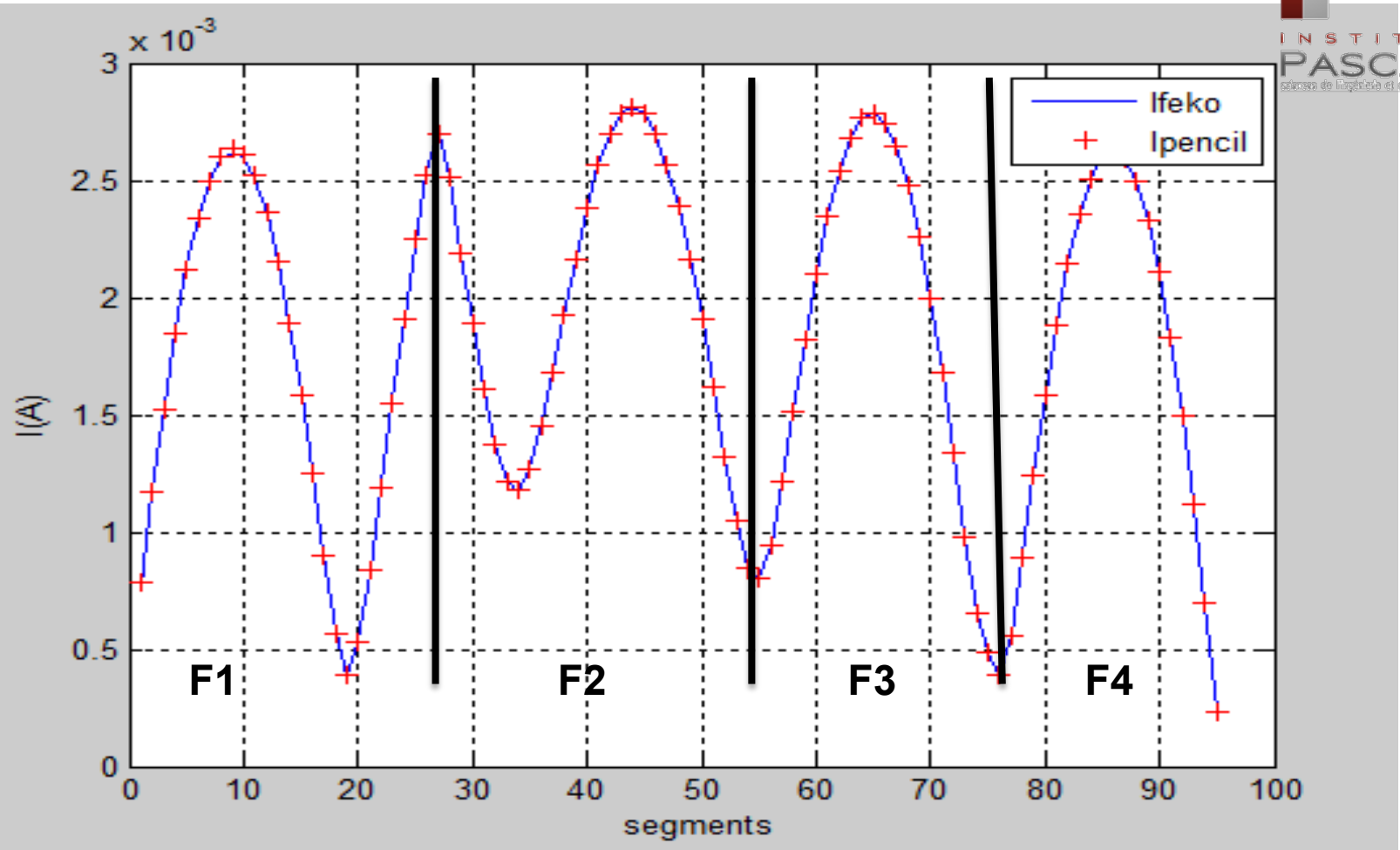


**Excellent agreement between Feko results and results reconstructed by MPM method for each branch F**

# Total and partial Electrical Field

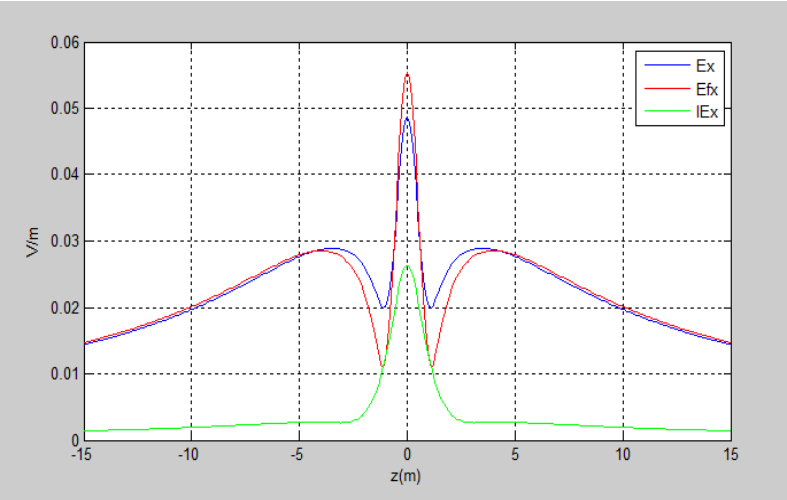


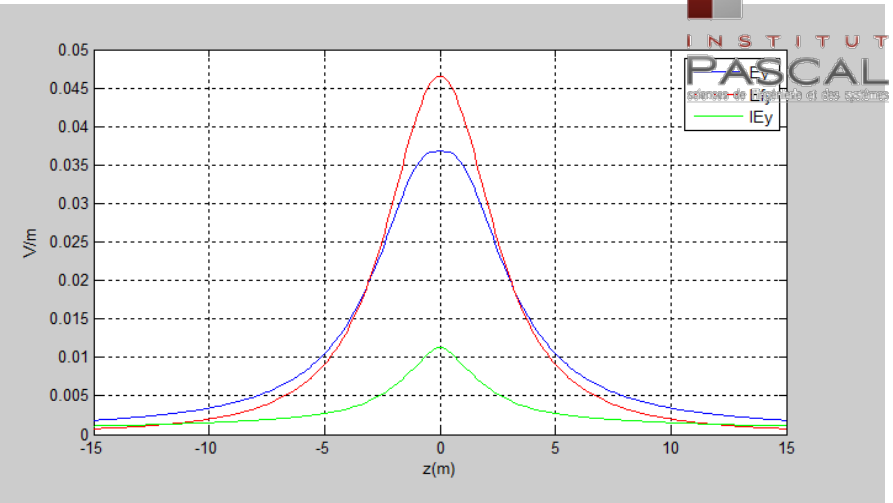


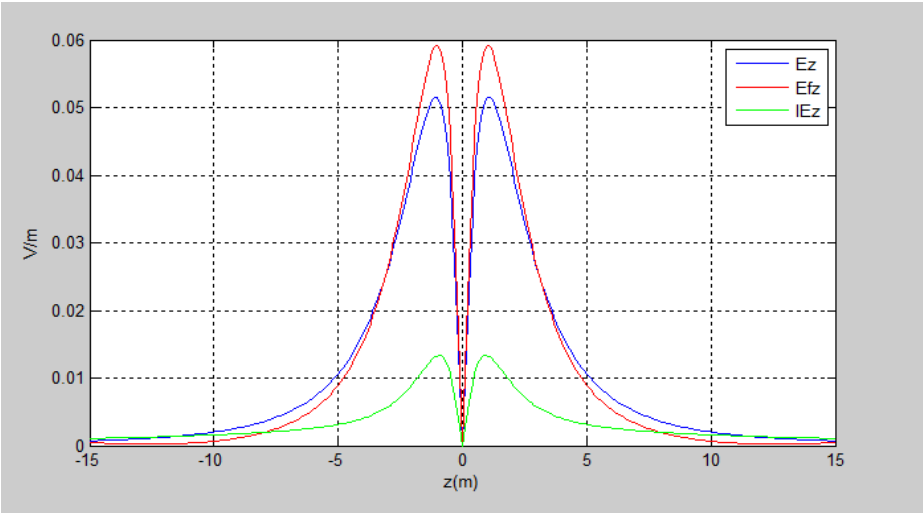


**The integral part can be neglected**

# Total and partial Magnetic Field

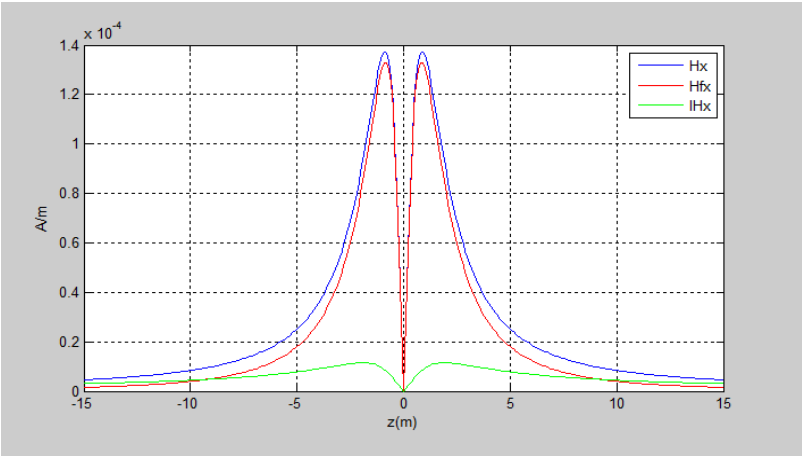


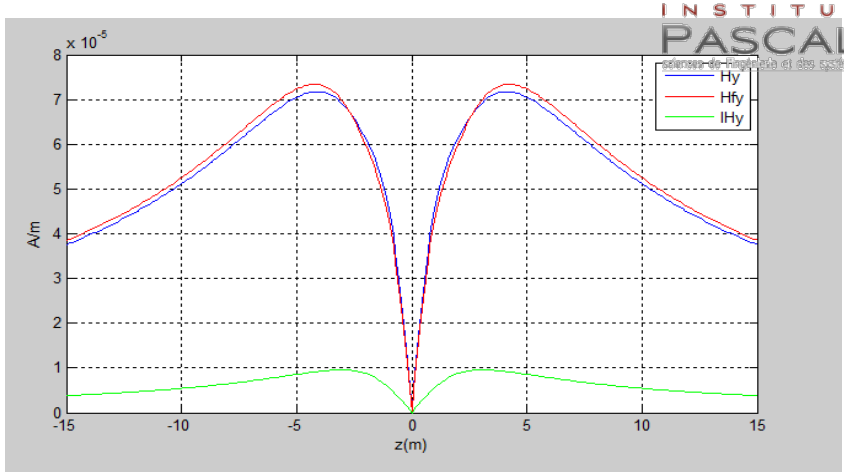


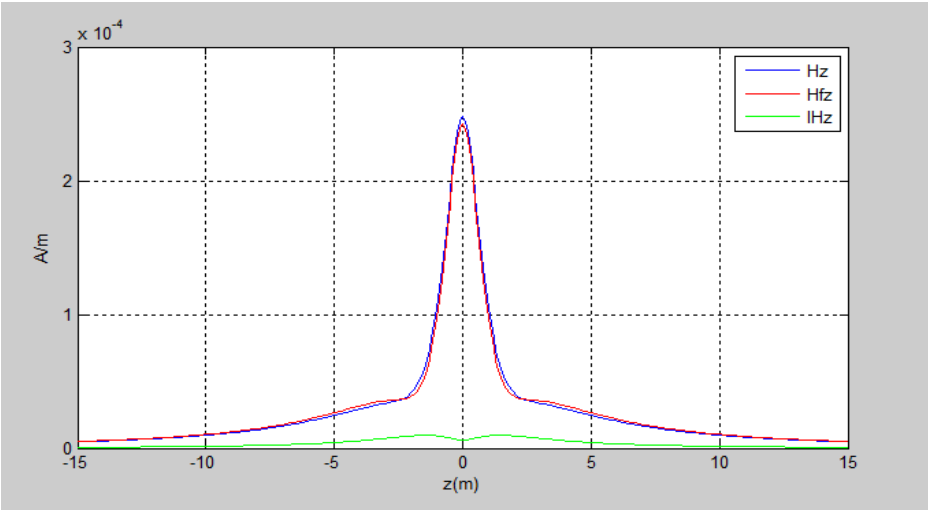


**The integral part can be neglected**

# U-shape of two-wire line

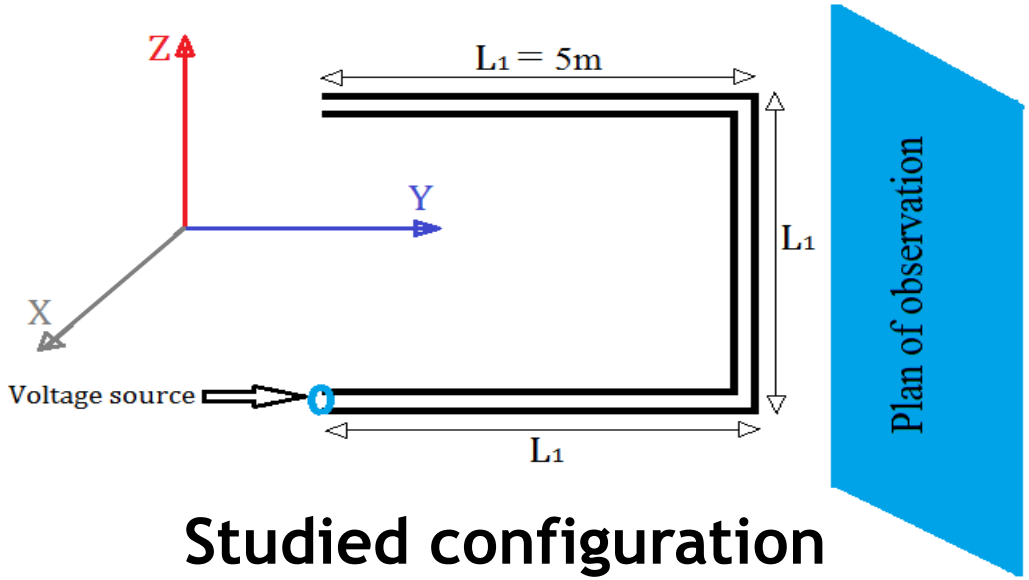


**Studied configuration**

Source of 1 V and 20 Mhz of frequency and 5 cm distance between conductors.

**The observation points are defined as follows:**

y varying between -1 m and 7 m, z varying between -2 and 7 m, with x = 1 m, we choose these region in which the radiated field is high enough.

# Radiated EM field

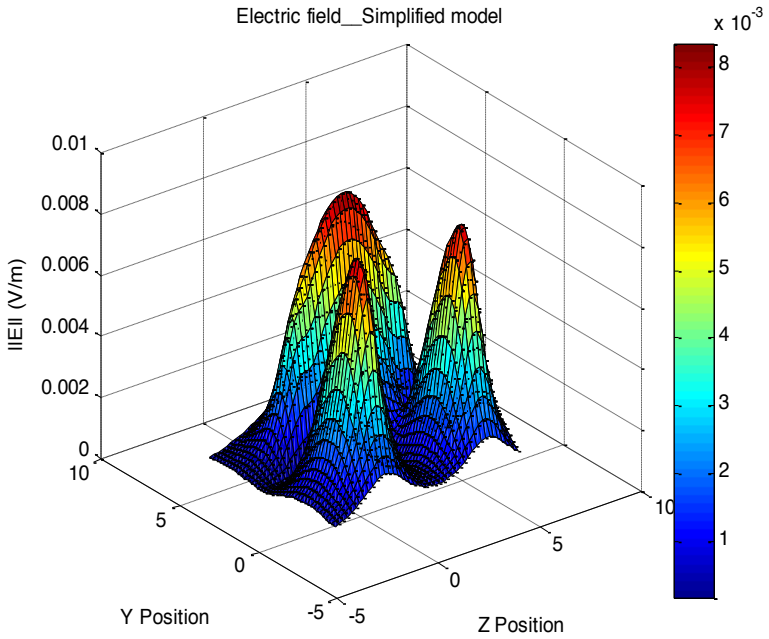


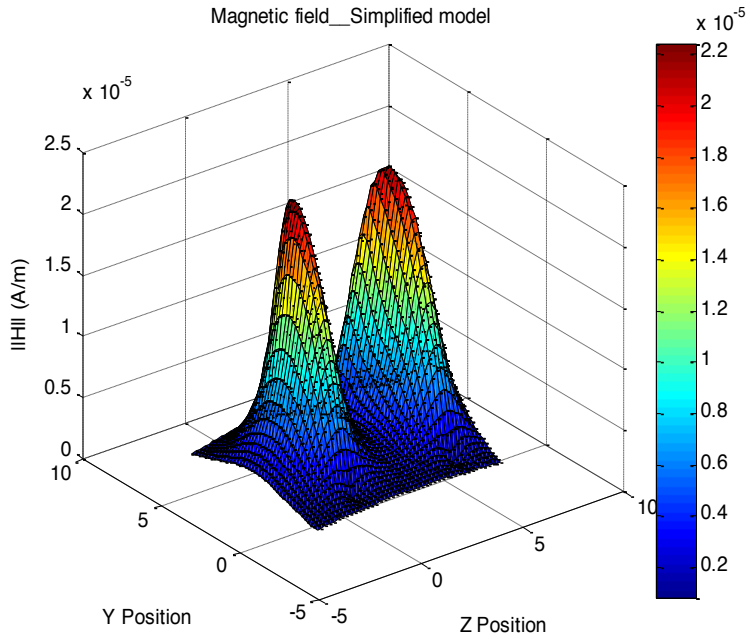


**Electric field estimated by our approach and by Feko**

*Error less than 4%*

**Magnetic field estimated by our approach and by Feko**

*Error less than 4%*

# Influence of the coupling on the EM field

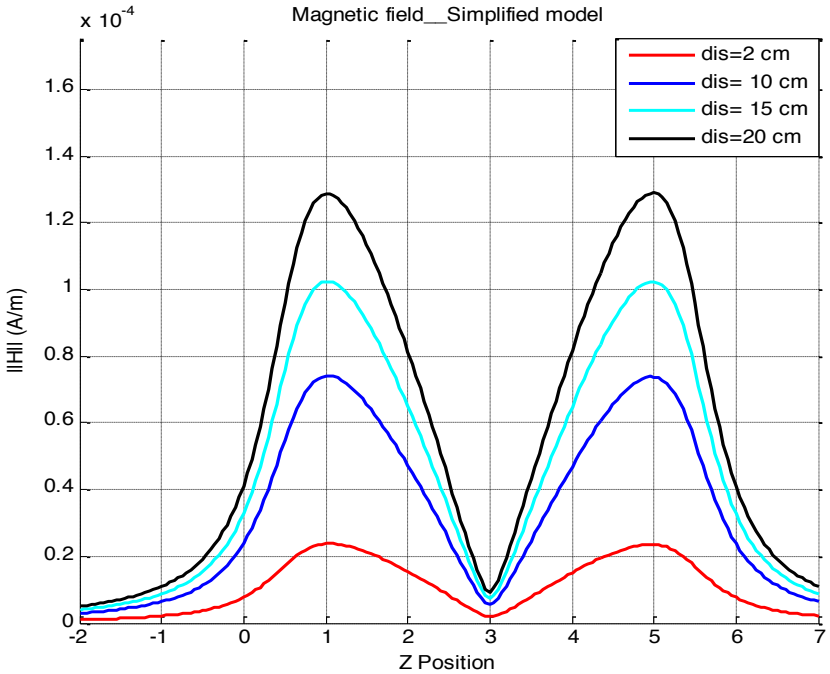


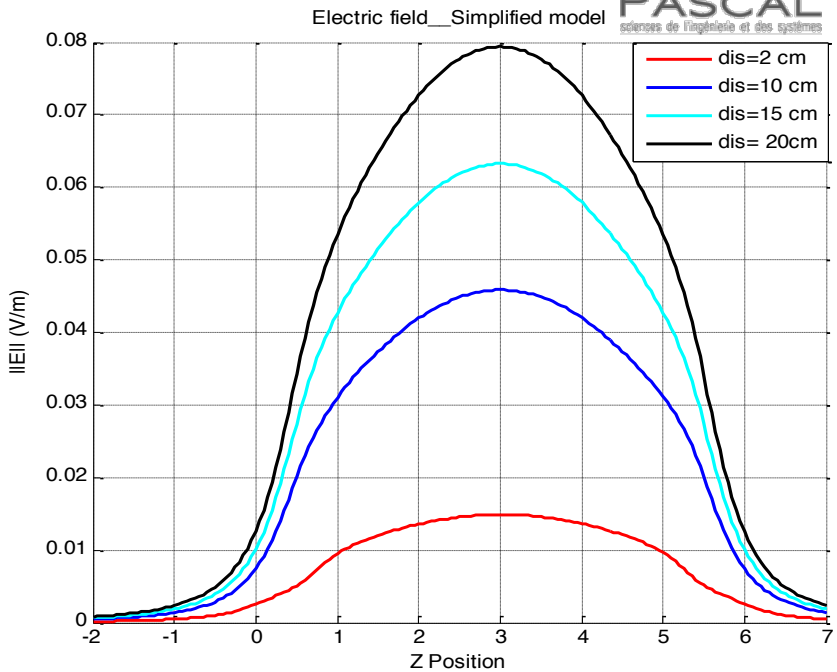


**Influence of the coupling on the magnetic field**

**Influence of the coupling on the electric field**

The observation points P (x, y, z) are:
x = 20 cm, y = 50 cm, z between -2 m and 7 m with a step of 10 cm

# Experimental setup

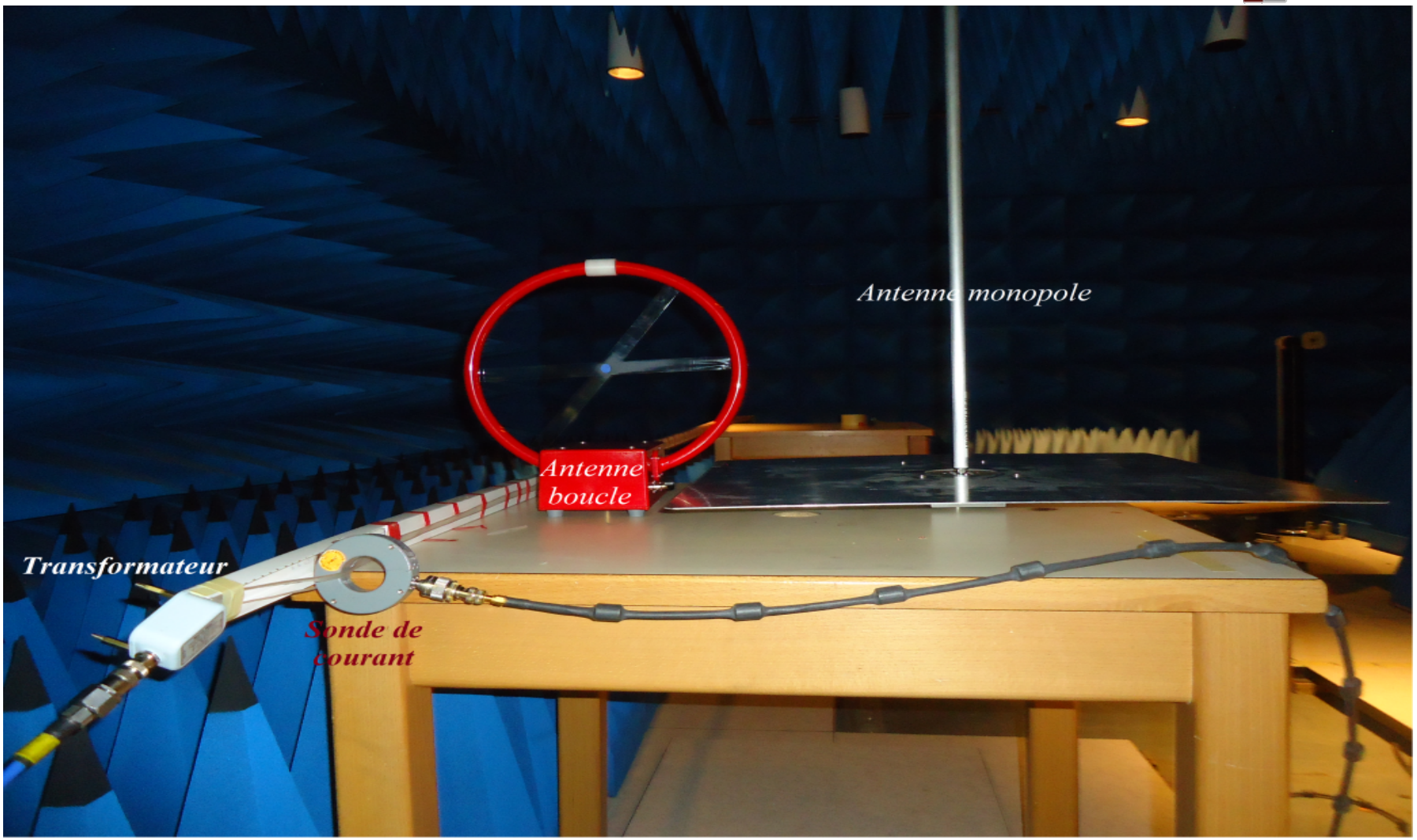

# Measurement results

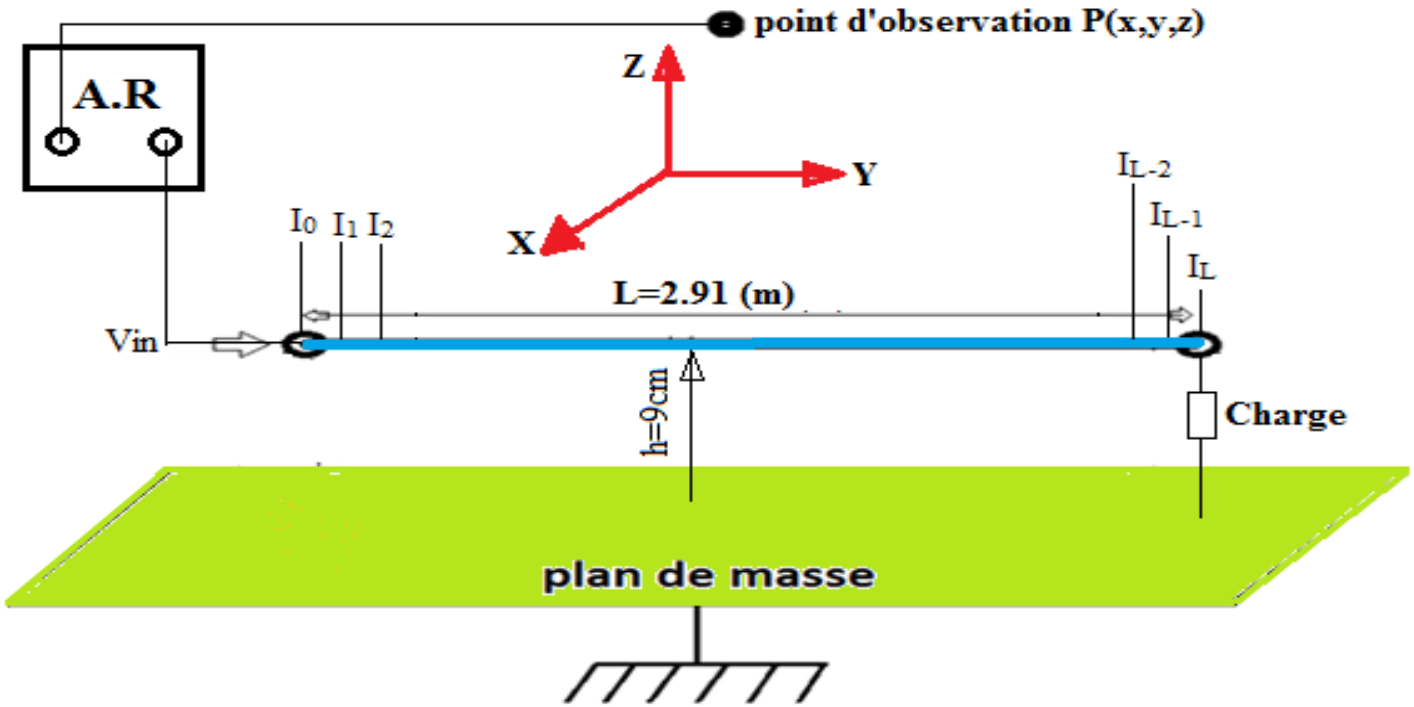


**Single-line parallel to a ground plane**

# Current and magnetic field

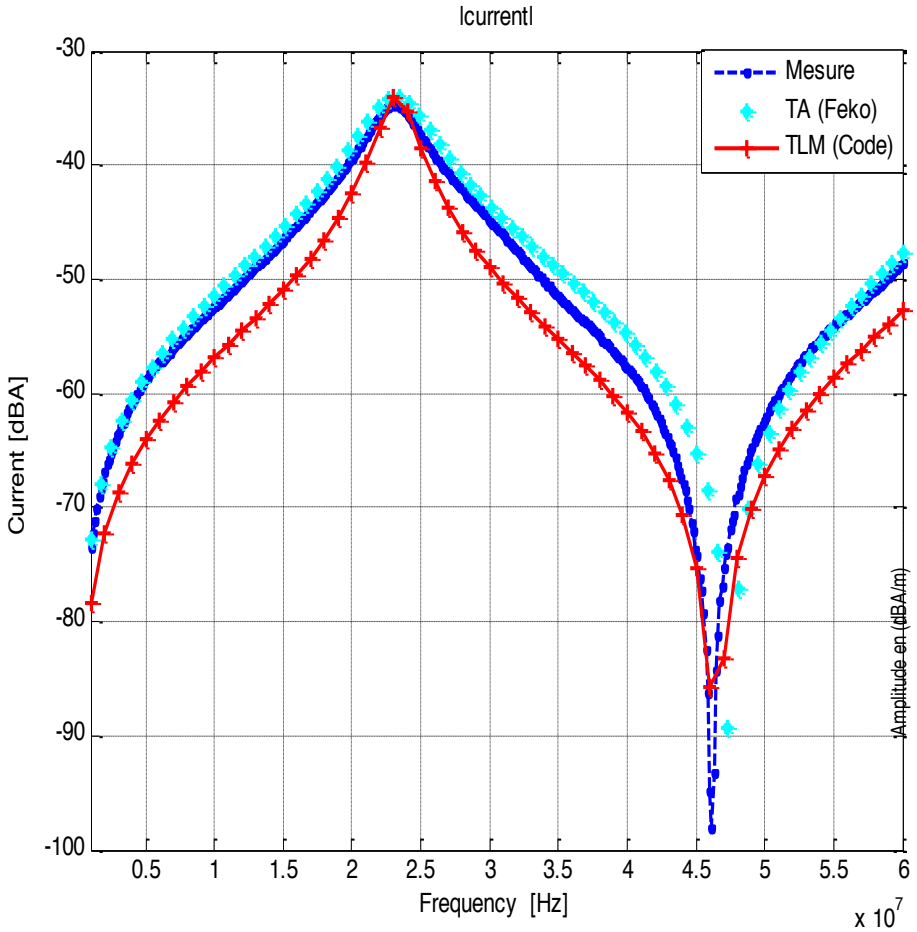


$$\begin{cases} x = 0.25(m) \\ y \in [0.1(m), 3(m)] \\ z = 0.11(m) \end{cases}$$

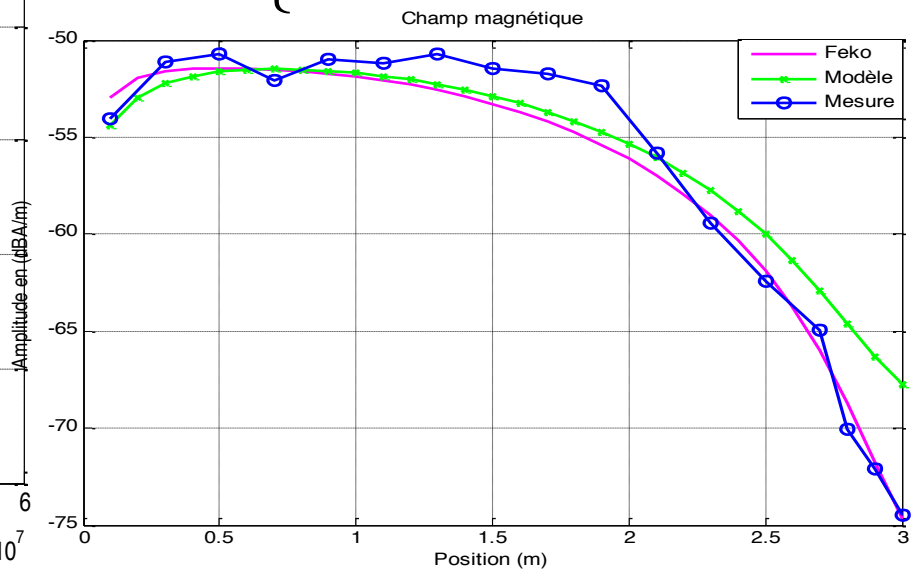


**Near end current in frequency domain**

**Magnetic Field depending on observation point**

# Electric and magnetic field

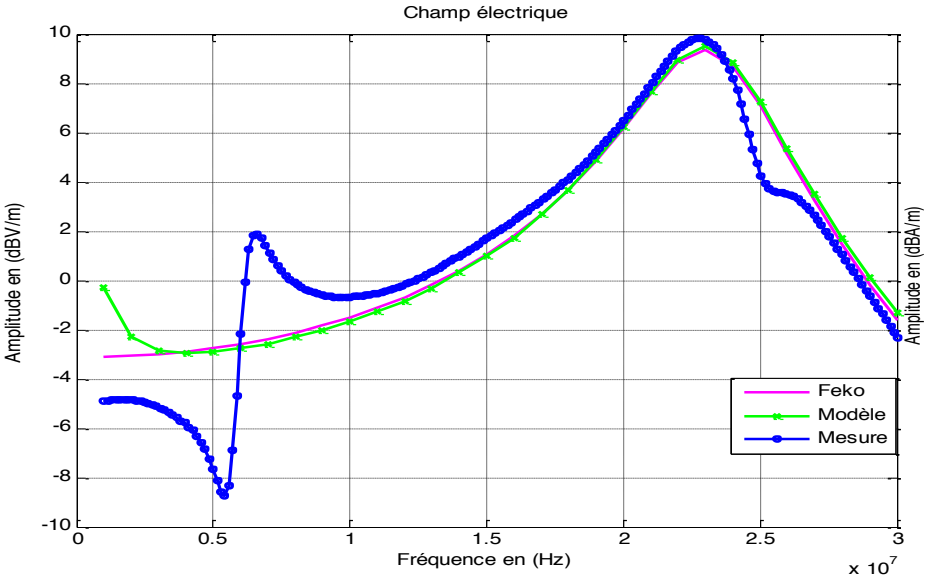


Electric Field
in frequency domain

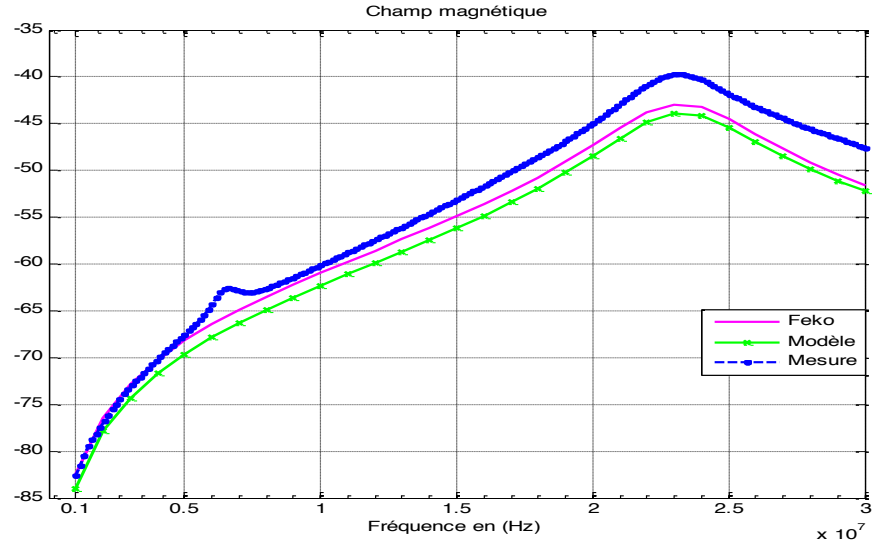


Magnetic Field
in frequency domain

# Conclusions and on-going work

- Analytical model based on discontinuities (electrical and geometrical) currents and there two first derivatives,
- Short computing time to evaluate radiated near and far field,
- Simulation and measurement results agree satisfactory,
- **Sensor less EM Field setup based only on discontinuities current measurements (PostDoc 2018).**

Clermont Auvergne University
Sungkyunkwan University

# Efficient characterization of scattering objects in the frequency domain

PhD: Mahmoud KHODJET-KESBA (2014)

# Introduction

## ❑ Autonomous vehicles:


## ❑ Collaboration between:

- Pascal Institute of Blaise Pascal University (France)
- Intelligent Systems Research Institute of Sungkyunkwan University (South Korea)

# Introduction

- The UWB radar use short pulses

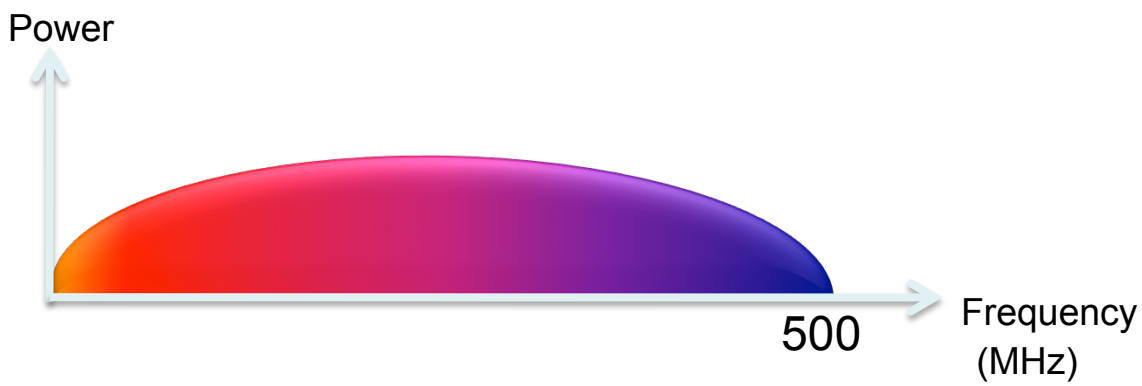


- High resolution for distance
- Enhance targets identification
- Simple implementation and lower costs

# Natural complex resonances

**The scattered signal in the time domain is composed of two parts:**

- **impulsive component,**
- **a damped oscillatory component.**

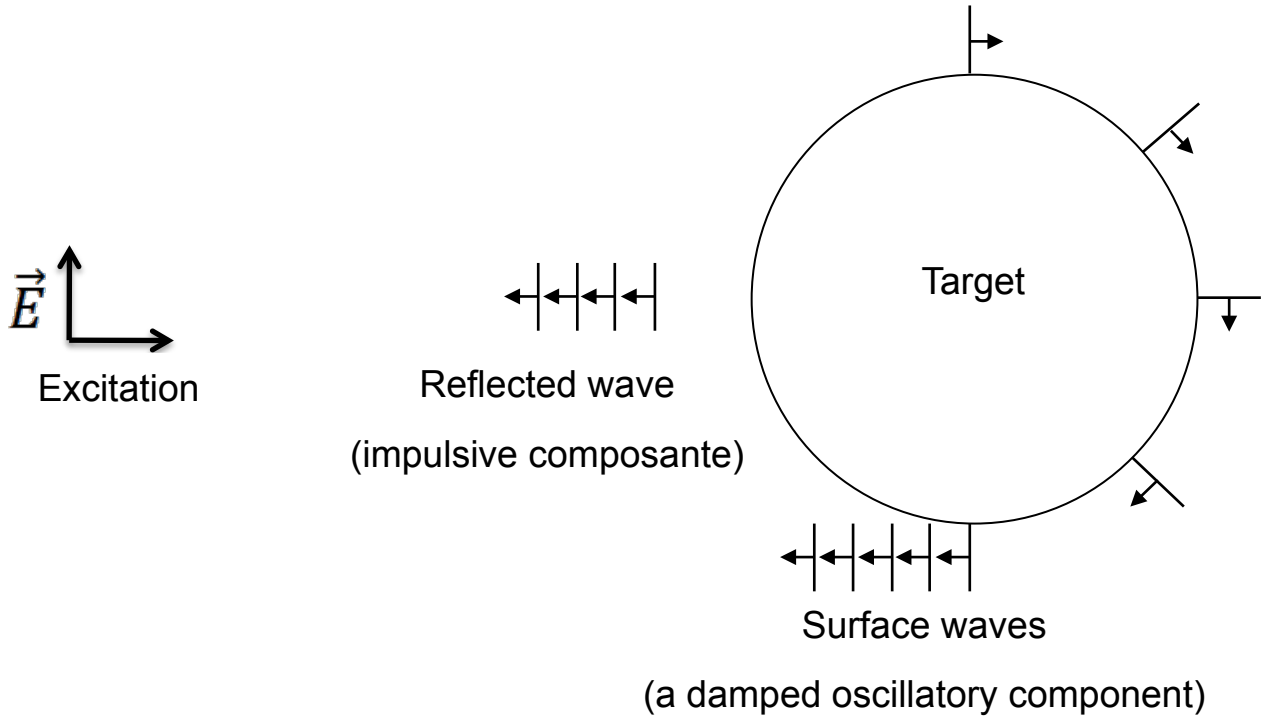

# Natural complex resonances

## Case of conducting sphere:

- The backscattered field by a sphere is given by:

$$E^s = E_0 \frac{e^{-ikr}}{2kr} \sum_{n=1}^{\infty} \frac{(-1)^n (2n+1)}{\hat{H}_n^{(2)\prime}(ka)\, \hat{H}_n^{(2)}(ka)}$$

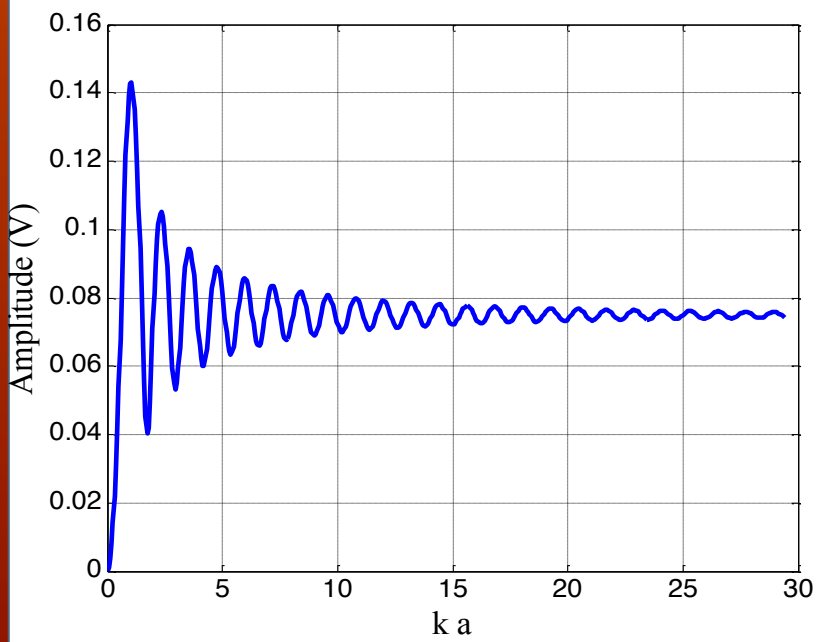


**Amplitude of the backscattered Field from a sphere**

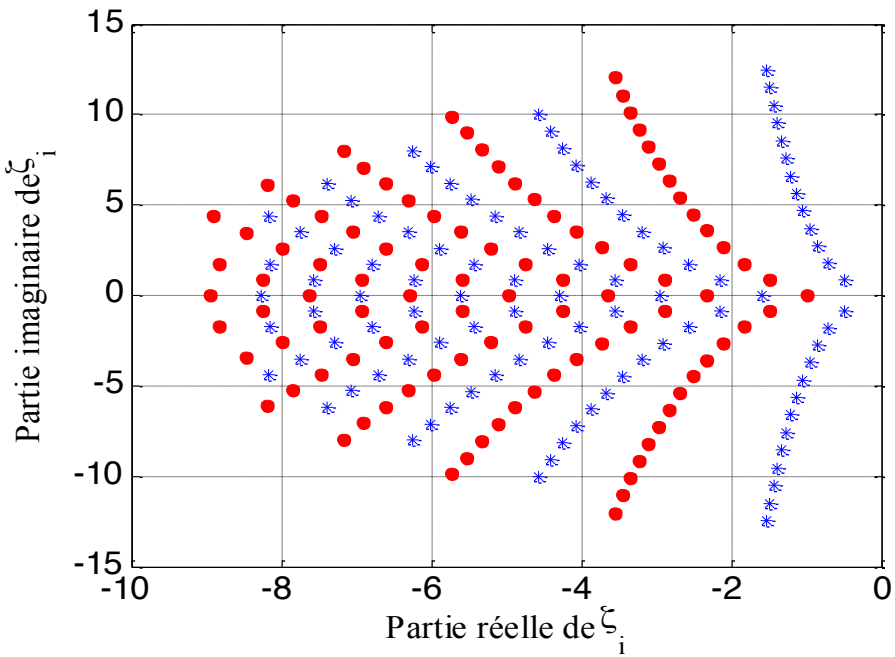


**Natural complex resonances of a sphere**

# The backscattered field from a conductive sphere

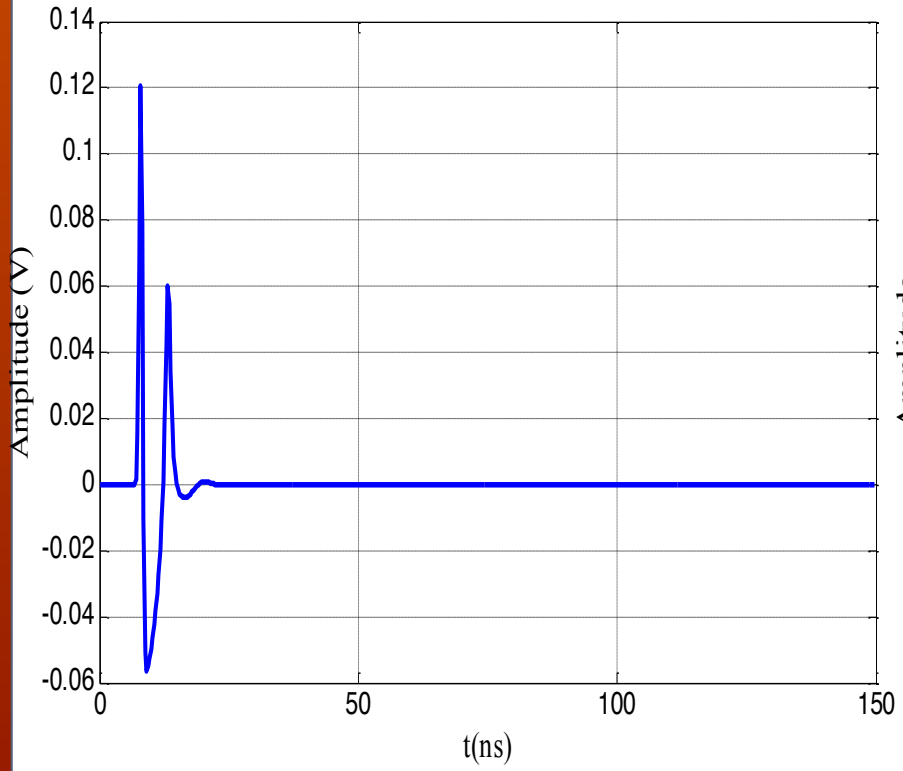


In time domain

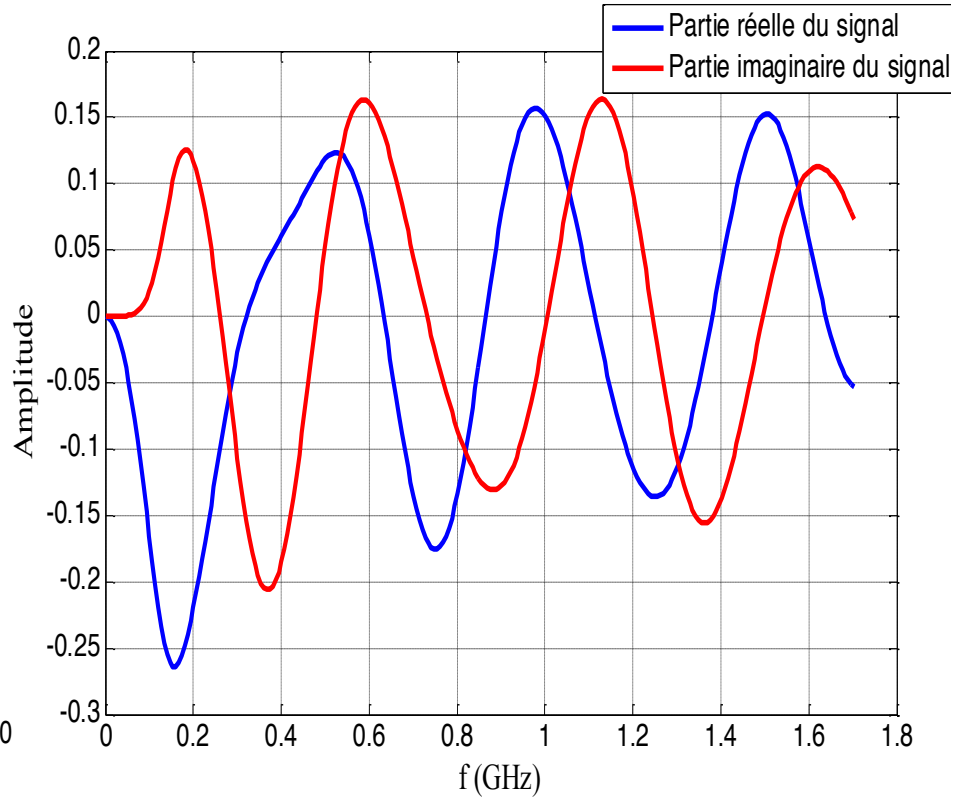


In frequency domain

The backscattered field from the sphere (radius of 30 cm)

# Identification chronogram

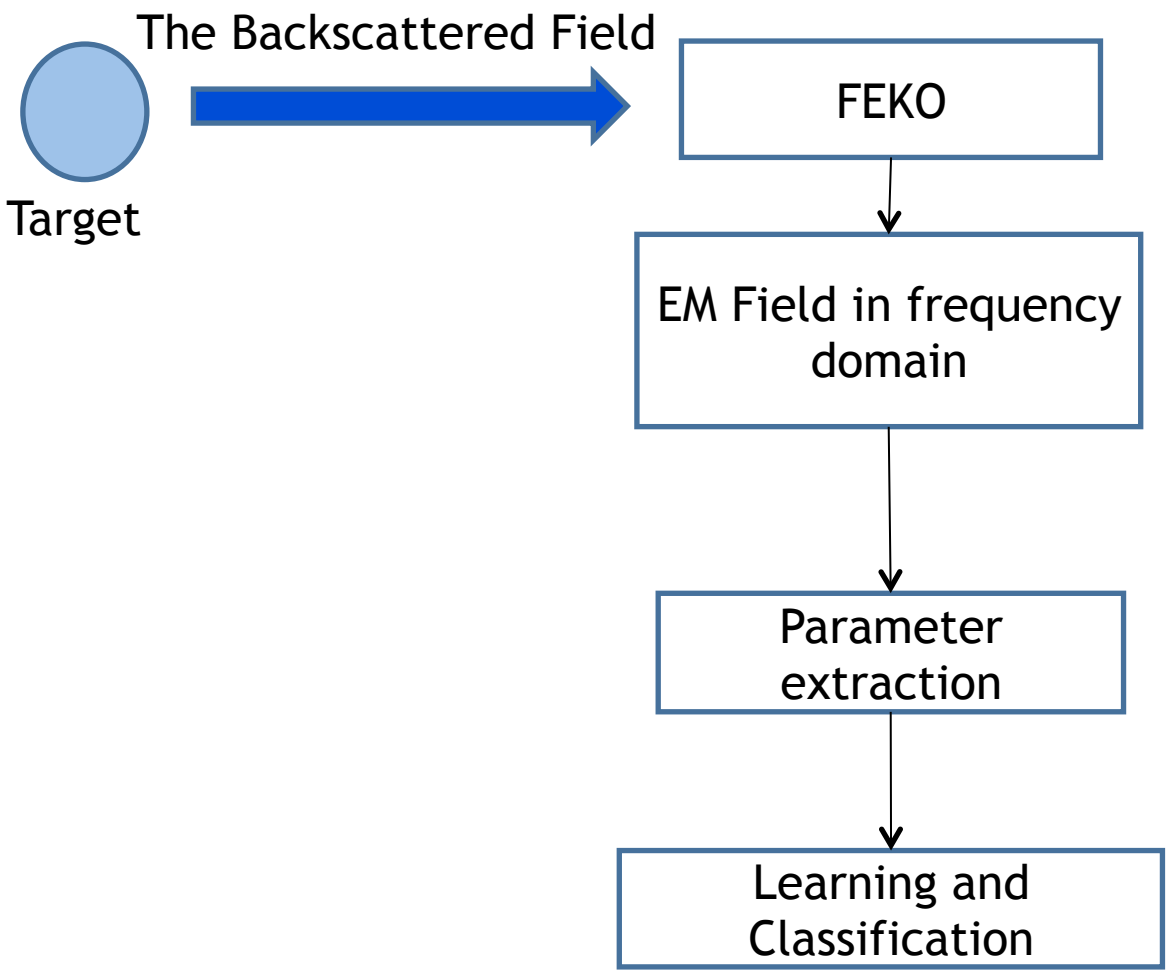

# Supervised classification

## Definition:

- Supervised classification is based on a database of training data to automatically generate rules for grouping of individual data into a number of classes. We chose three methods to achieve this classification.

- The classification is done in two steps:
  - Learning step,
  - Test step.

# Simulation results

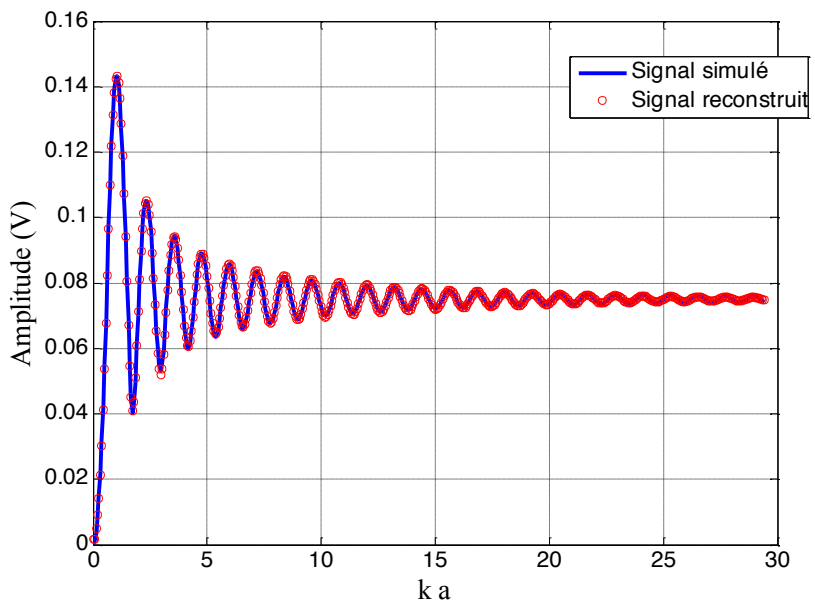


Amplitude

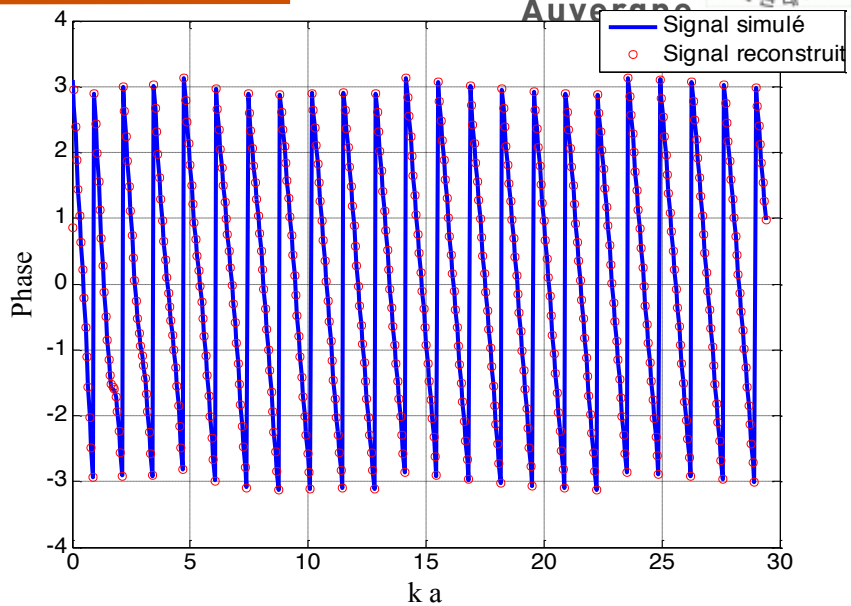


Phase

## Reconstructed and simulated signals

| Poles $(\gamma_n - t_n j)$ | Residus $(b_n(r))$ |
|---|---|
| -2.0289 - 13.487 j | -0.0142 - 0.0192 j |
| -0.1252 - 9.8605 j | 0.0179 - 0.0091 j |
| -0.6280 - 9.6984 j | 0.0724 - 0.0101 j |
| -1.8427 - 6.4904 j | -0.1326 - 0.0019 j |
| -0.4937 - 4.7976 j | -0.0168 + 0.0375 j |
| 0.0001 - 4.6683 j | 0.0745 + 0.0045 j |

# Simulation results

**Classification of canonical objects of different sizes:**

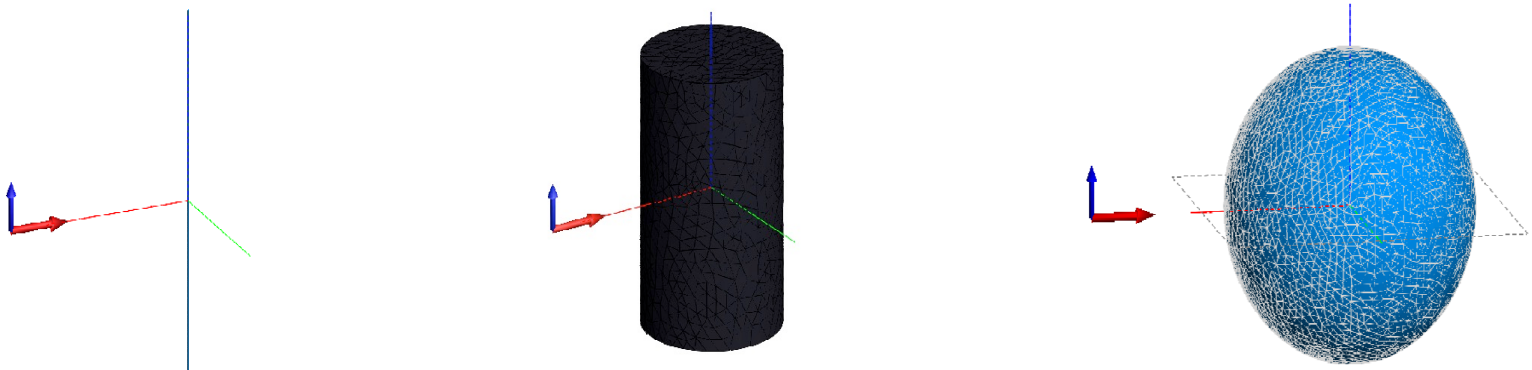

- In total, we have 24 objects to be classified:
- Wire : l= 1, 1.3, 1.5, 1.7, 2, 2.4, 2.5, 3, and radius r= 0.0025 m
- Sphere : r= 0.15, 0.2, 0.28, 0.3, 0.35, 0.4, 0.45, and 0.5 m
- Cylinder : l=0.4 and r=0.17, l=0.4 and r=0.23, l=0.5 and r=0.15, l=0.5
- and r=0.25, l=0.6 and r=0.2, l=0.7 and r=0.1, l=0.8 and r=0.19, and l=1 and r=0.15 m

| Classification methods | Naïve Bayes | K-NN | | | SVM |
|---|---|---|---|---|---|
| | | K=1 | K=3 | K=5 | |
| Classification accuracy | 100 % | 100 % | 91.67 % | 91.67 % | 100 % |

# Simulation results

**Classification of complex objects with different SNR and different excitation angles:**

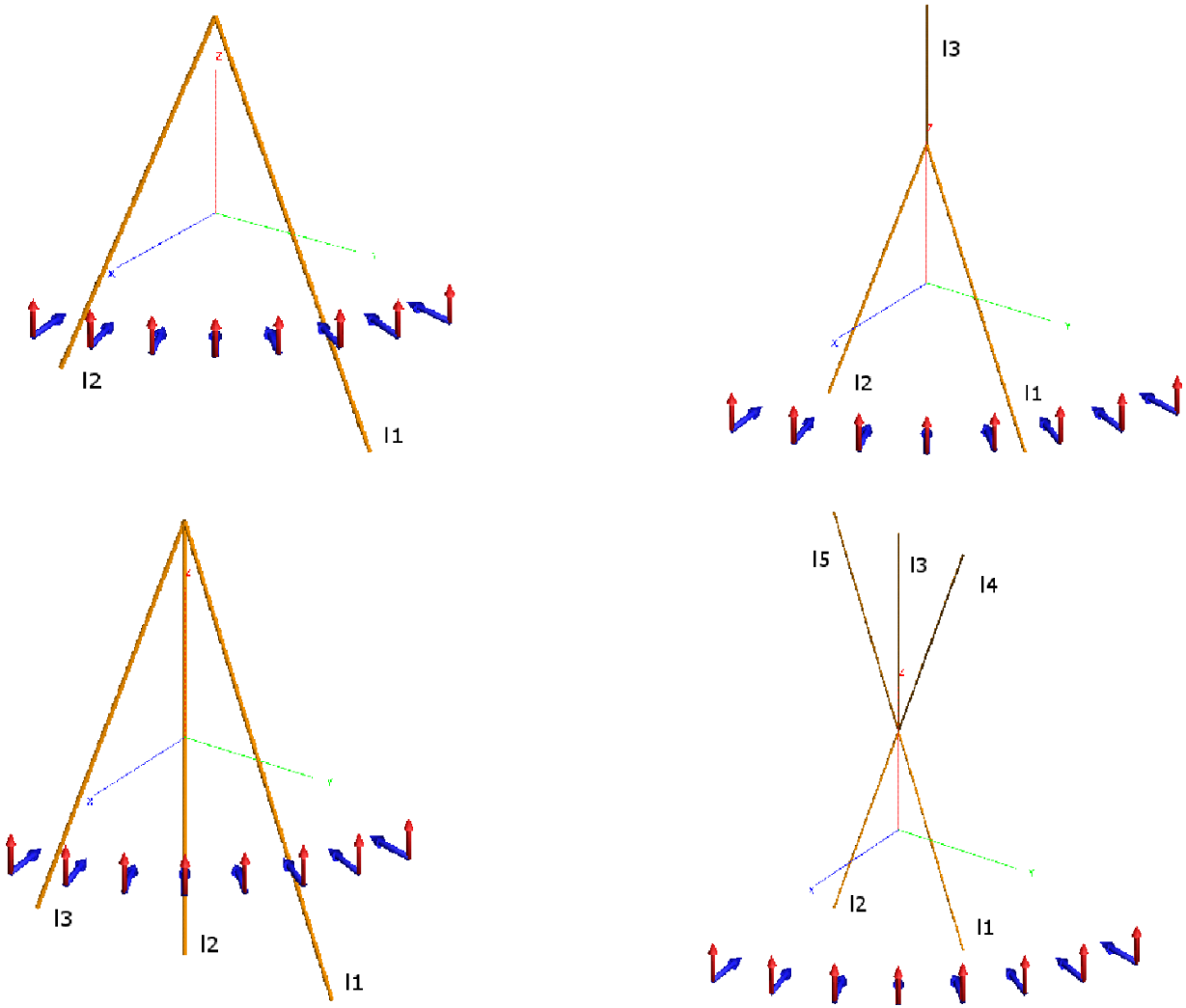

# Simulation results

**Learning data:**

- 8 angles: 5, 15, 25, 35, 45, 55, 65 et 75°
- 20 measurements with SNR of 10 dB for each angle
- In total: 4 x 8 x 20 = 640 learning data

**Test data using only component $E_\theta$:**

- 8 angles: 5, 15, 25, 35, 45, 55, 65 et 75°
- 7 values of SNR: 0, 5, 10, 15, 20, 25 et 30 dB for each angle
- 80 measurments for each SNR
- In total: 4 x 8 x 7 x 80 = 17 920 data to test

| SNR (dB) | 0 | 5 | 10 | 15 | 20 | 25 | 30 |
|---|---|---|---|---|---|---|---|
| K-NN (K=3) | 71.33 % | 80.74 % | 93.83 % | 96.48 % | 97.66 % | 98.52 % | 99.30 % |
| NB | 58.98 % | 74.84 % | 86.64 % | 87.03 % | 87 % | 87.07 % | 86.29 % |
| SVM | 73.95 % | 81.37 % | 94.45 % | 97.58 % | 99.41 % | 100 % | 100 % |

# Conclusions and perspectives

- We have proposed in this part to identify scattering objects with a small number of signatures (singular values, poles, residues).
- The integration of these signatures in complex systems should help to model completely and with limited numerical effort.
- These signatures are enough to effectively classify three families of four canonical objects and complex objects.
- The use of all components backscattered field effectively increases the classification.
- Use both transmit polarizations would add new EM components in the data and make the classification more robust .

# Smart Metering

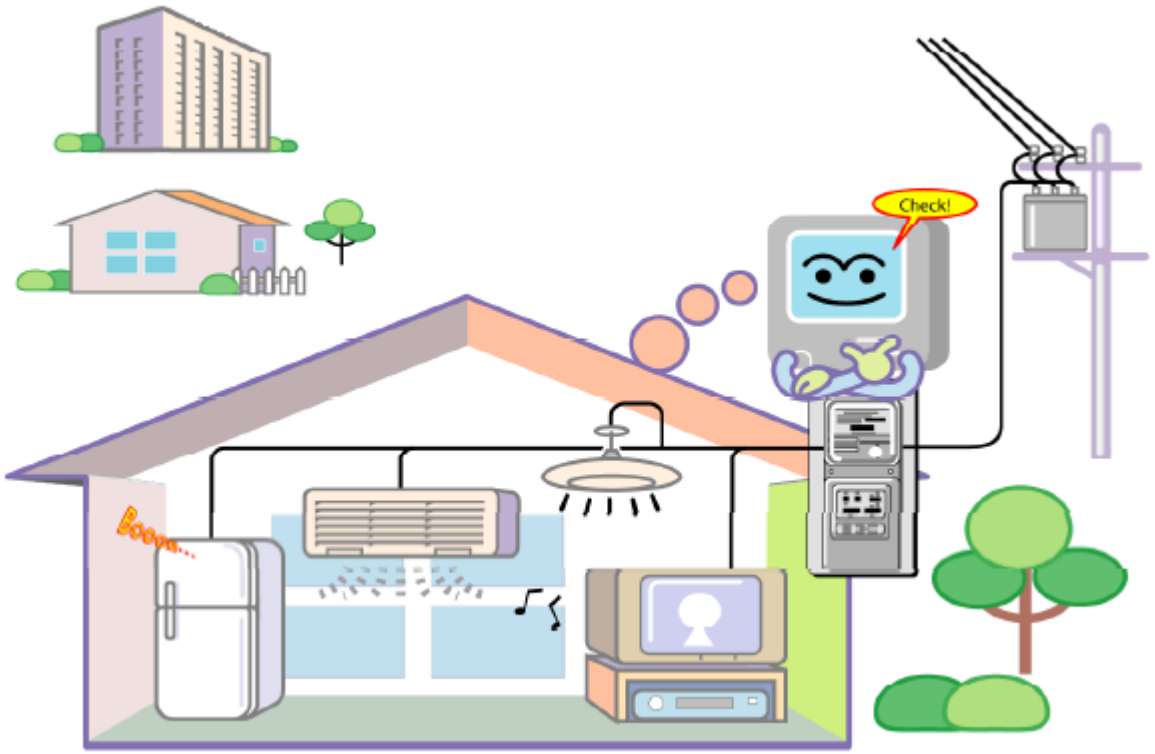


**PhD: Hala Najmeddine (2009)**

# Smart Metering

Objective of load monitoring:

- **Regulate** the energy consumption.
- **Determination** of the operation schedule of individual appliances and their energy consumption.

- Non intrusive: No intrusion into the energy consumer's property.
- Allows the identification by the matrix pencil method (**in time domain**) of the consumption of electrical loads without intervention on individual loads.

# Active power based on poles and residues

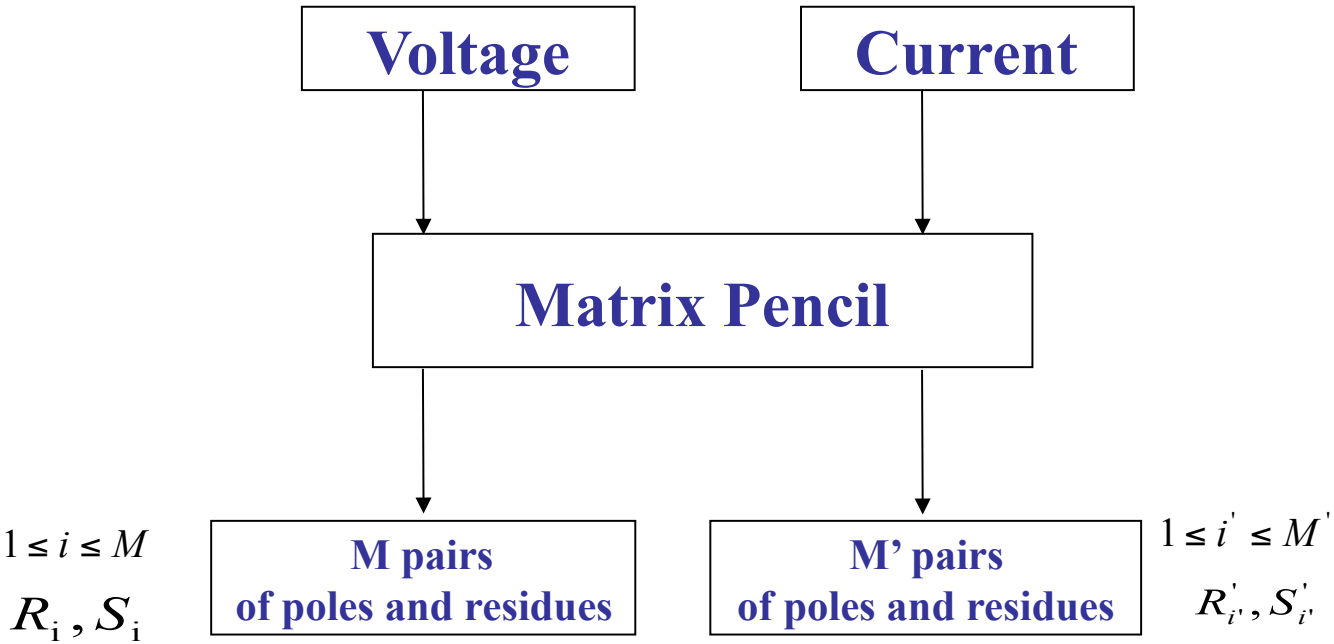


$$P = \sum_{i=1}^{M} \sum_{i'=1}^{M'} R_i R'_{i'} e^{(S_i + S'_{i'})T/2} \quad \text{sinhc}\left[(s_i + s'_{i'})T/2\right]$$

# Non-Intrusive Appliances
# Load Monitoring method

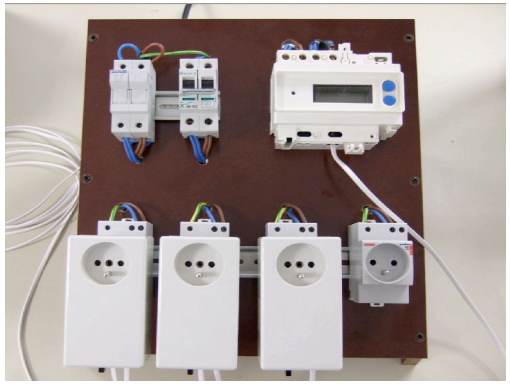

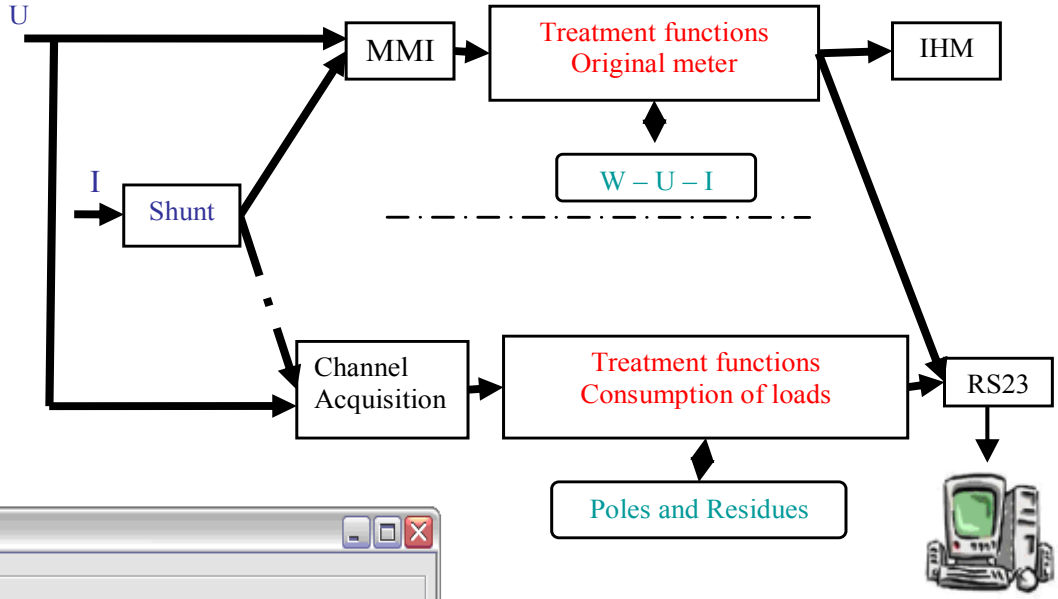


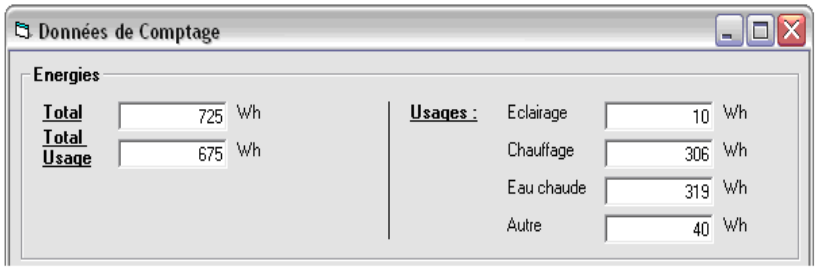

# Experimental Results

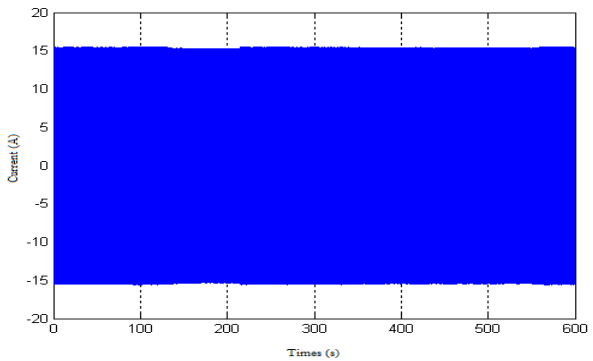


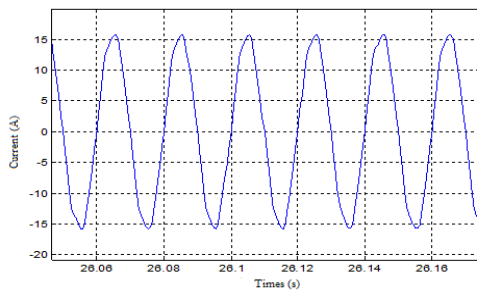


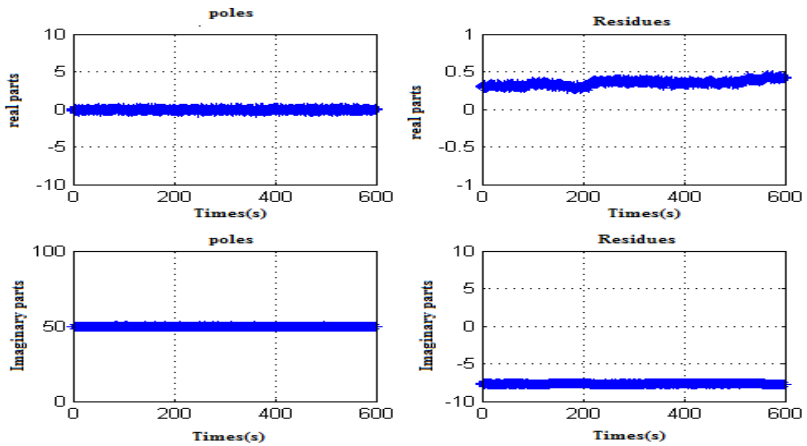


$$S = \frac{j\omega}{2\pi} = 0 + 50j$$

$$R = \frac{E\sqrt{2}}{2r.j} \approx 0 - 7.7j$$

# Experimental Results

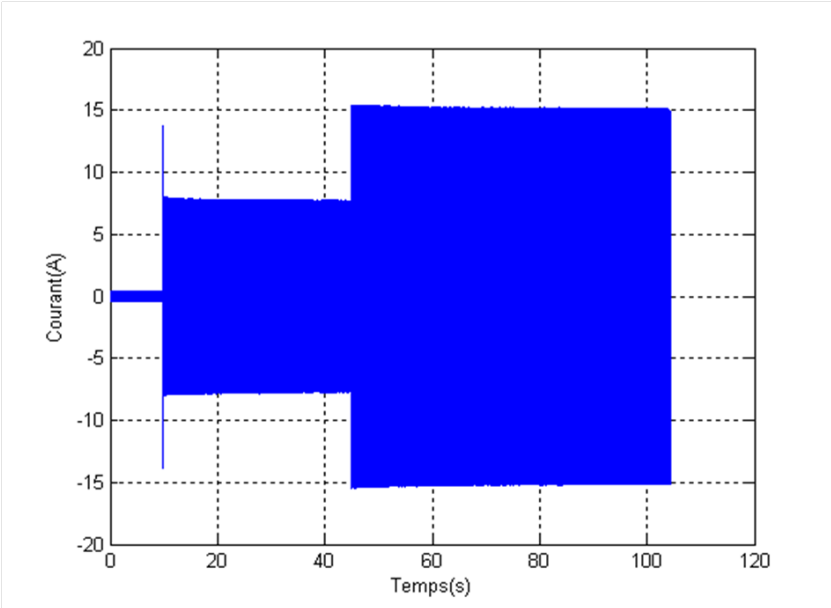


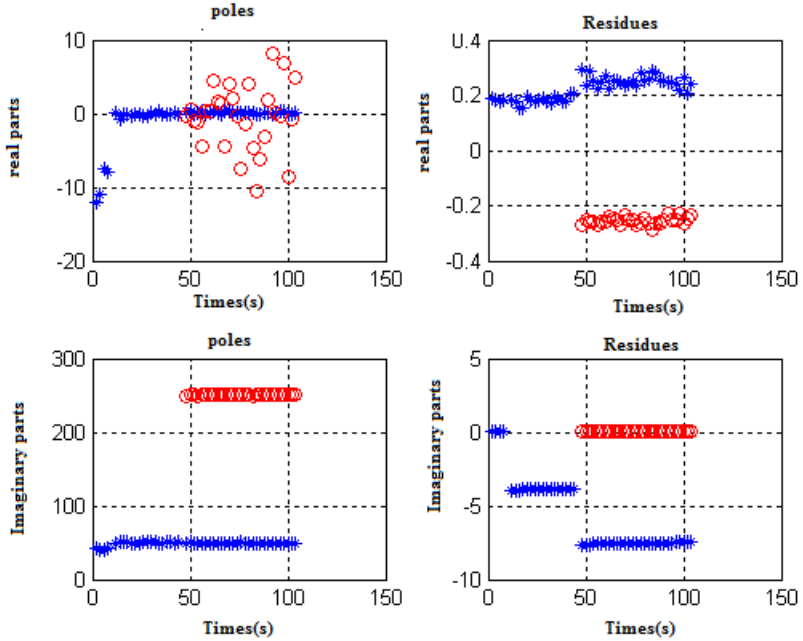

# Conclusions

- In this work, we present our contribution to Non Intrusive Appliance Load Monitoring.
- The MP method shows several advantages:
  - Robustness against measurement noises
  - Less data required to identify the original signal by using reduced number of poles and residues.
- Different **realistic case scenarios** have been studied and the results arising from this analysis seem to be rather **promising**,
- Moreover, this method also provides active power, reactive power and harmonic power in close form.
- The proposed method has been successfully integrated into a platform of a smart meter.
- This procedure has been patented nationally and internationally.

# Analysis of Electrophysiological activity by using MPM

PhD: Zied MIZOURI (2017)

**PEPS: First Support of Exploratory Project (June 2015-June 2016)**

[1]Institut Pascal, CNRS-UMR 6602
[2]Neuro-dol, Inserm U1107

# Peripheral nerves activity (ElectoNeuroGram)

## Analysis of peripheral nervous activity

1. Recording electrical nervous activity,
2. Extraction of field potentials or action potentials,
3. Identification of those responses by using Matrix Pencil method.

**Main goal: Recognition of the nociceptive response**

NEURO-DOL INSTITUT PASCAL

# Main objective

- Goal: Have a better understanding of **pain message** and **its propagation** from the peripheral to the central nervous system,

- Data base: **Electrostimulation** of sciatic nerve of rat,

- Proposal: **Stimulus artefact removal** using **Matrix Pencil Method** to focus only on useful information.

# Clinical context

- Neuron: Action potential

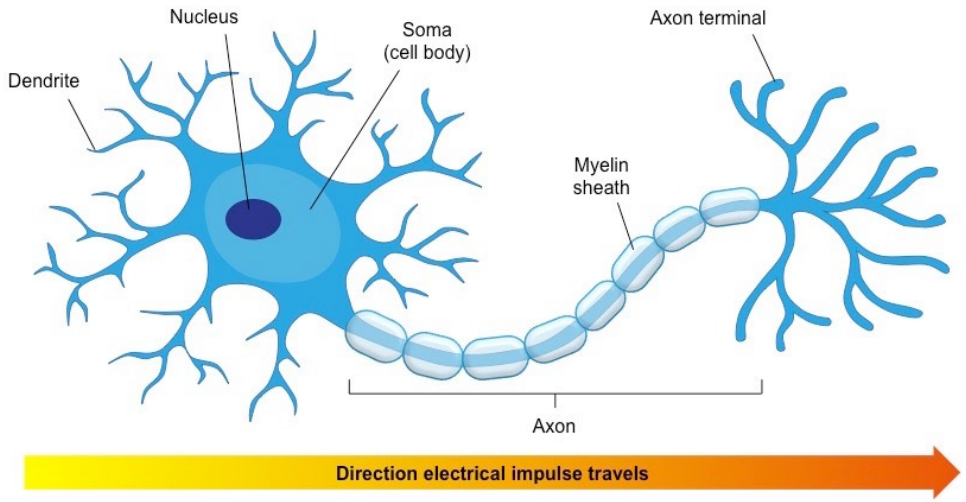


- Peripheral nerve: field potential (sum of individual neurons )

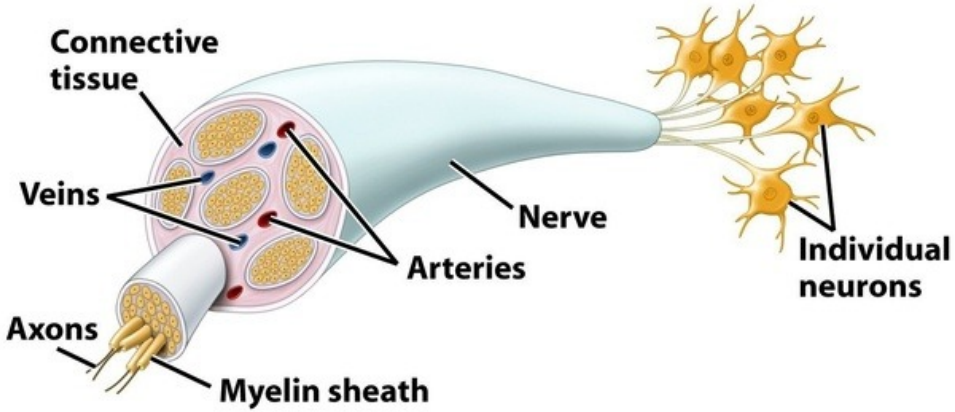

# Clinical context

- **Action potential:**

Existence of a gradient of concentrations and a gradient of charges.
Existence of leakage channels which makes the nerve fibre membrane permeable during stimulation.

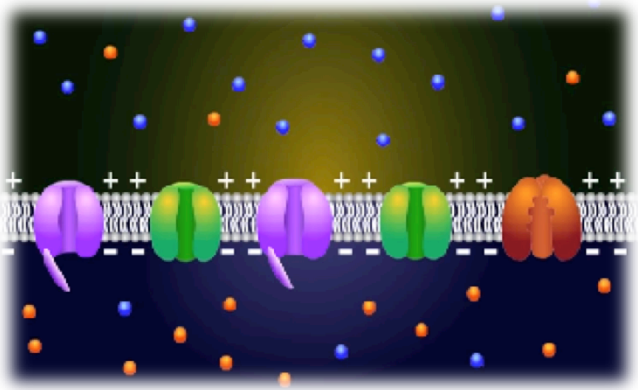

**Rest**

**Stimulation**

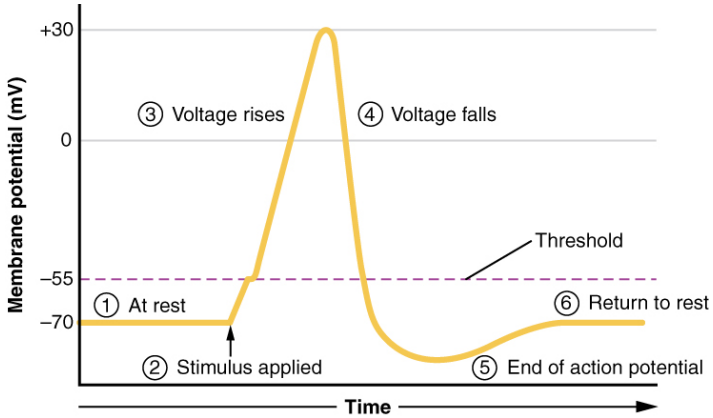


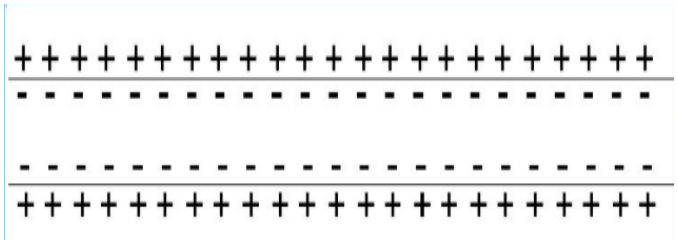

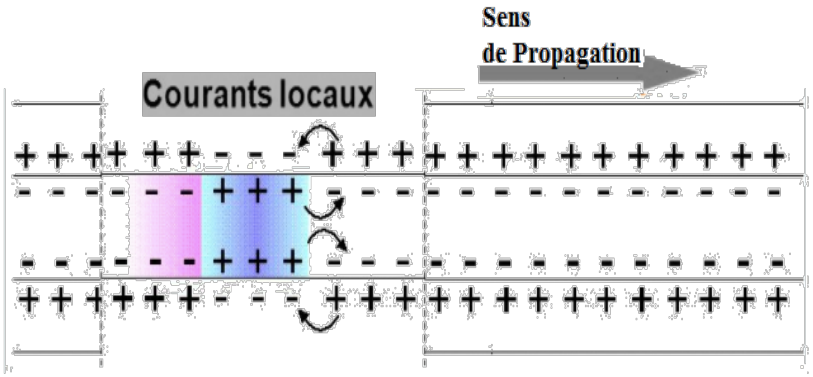

# Pathways of pain

Between painful message and perception of pain, we go through an electrochemical cascade, which can be summarized in 4 steps:

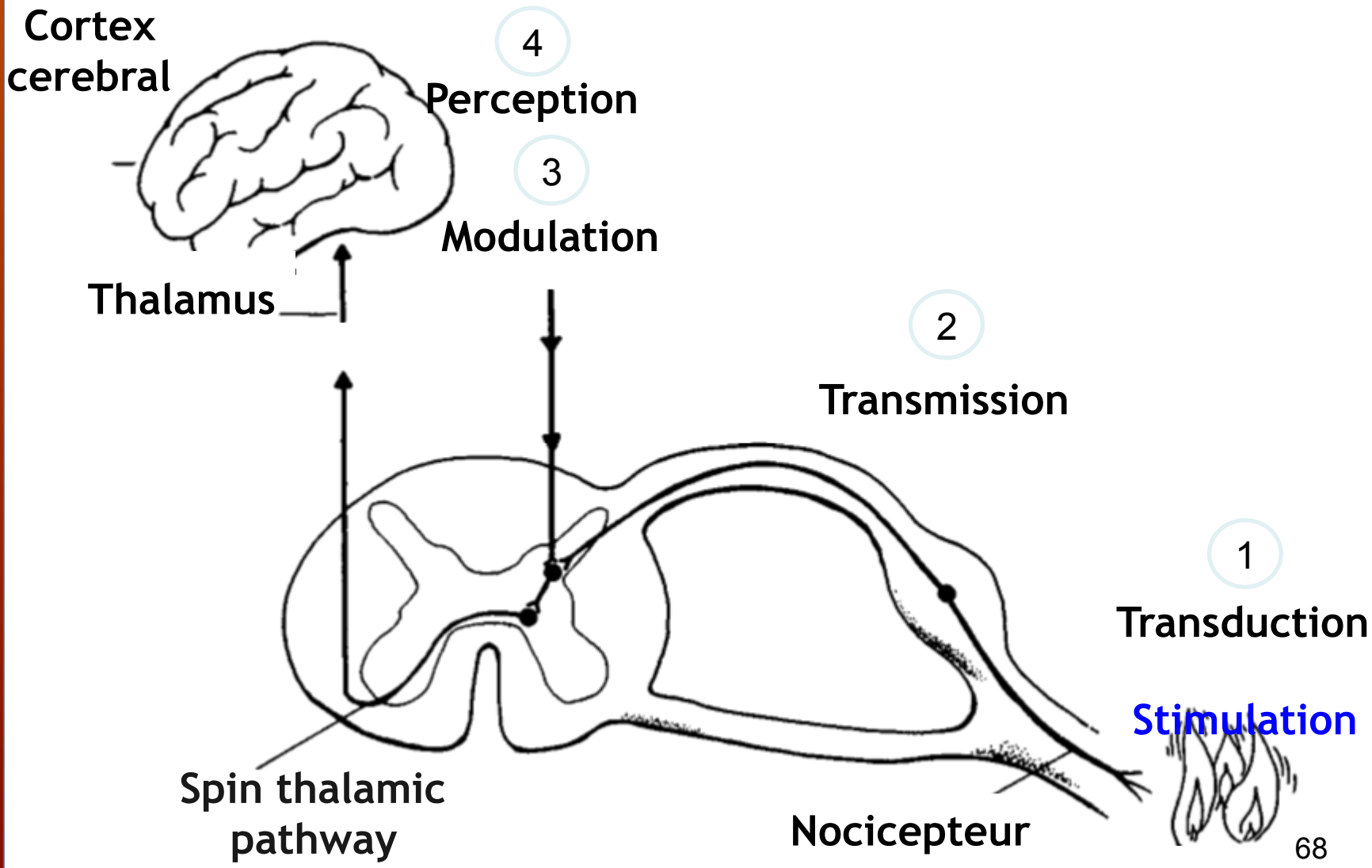

# Experimental setup

Diagram of Experimental procedure:

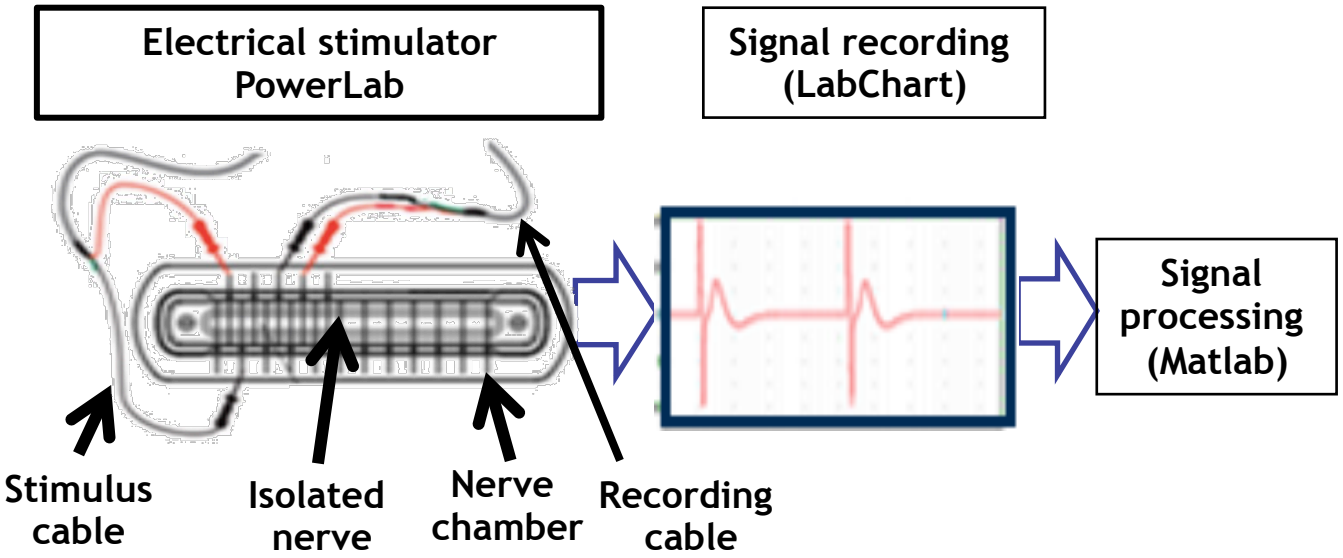


- Our data base is composed of signals recorded on the sciatic nerve of a rat,
- The electrodes used are invasive electrodes (to improve the selectivity of recorded signals: close to the source).
- These electrodes are directly connected to an amplifier equipped with a filter (high-pass and low-pass to eliminate unwanted frequencies).
- Stimulations ranged from 20mV to 400 mV (20mV step) ,
- Stimulus width from 200µs to 500µs.

# Process of extraction

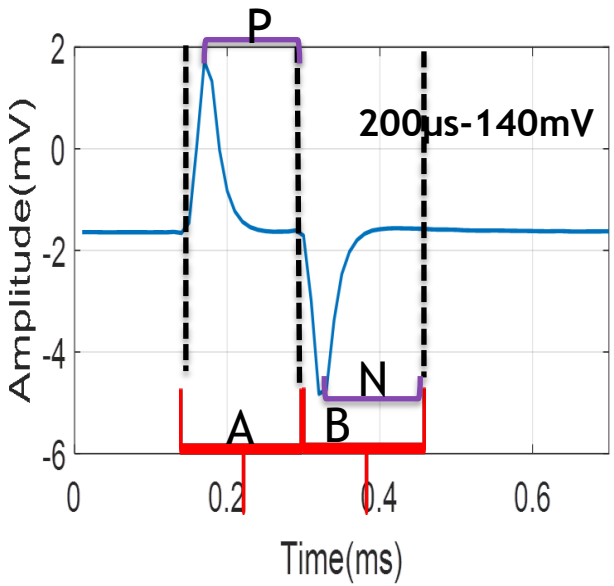


Fig.1 Stimulus artefact waveform

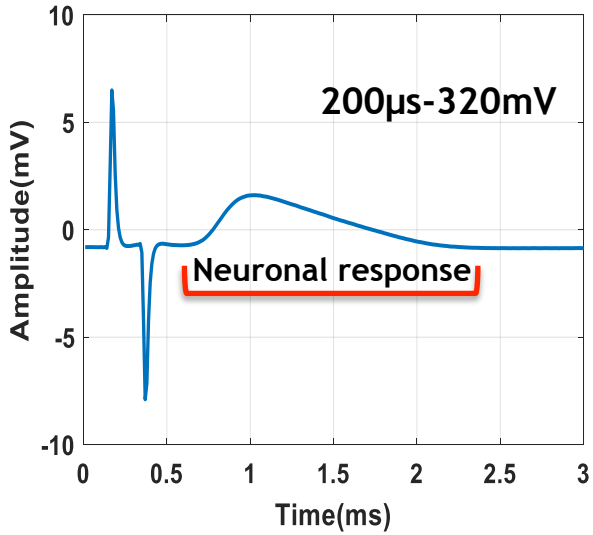


Fig.2 Example of signal with neuronal response

- Our method propose to decompose stimulus artifact into two symmetrical [A] an [B] parts (Fig. 1). In the case where stimulus artifact and response are clearly separated (Fig. 2)., the duration between artefact peaks allows us to ascertain the duration of [A] an [B] parts.
- Under the hypothesis that [A] and [B] are symmetrical, the proposed method reconstructed the exponential part (N) of [B] from the corresponding exponential decay part (P) of [A] and predict its evolution with the series of M damped exponentials.

# Numerical results

- **Case of stimulus artefact saturation:**

- Symmetry is not respected,
- Only exponential parts will be treated,
- In this case, we reconstructed the late part of exponential decay [$a_2$] from the window [$a_1$] (Fig. 3).

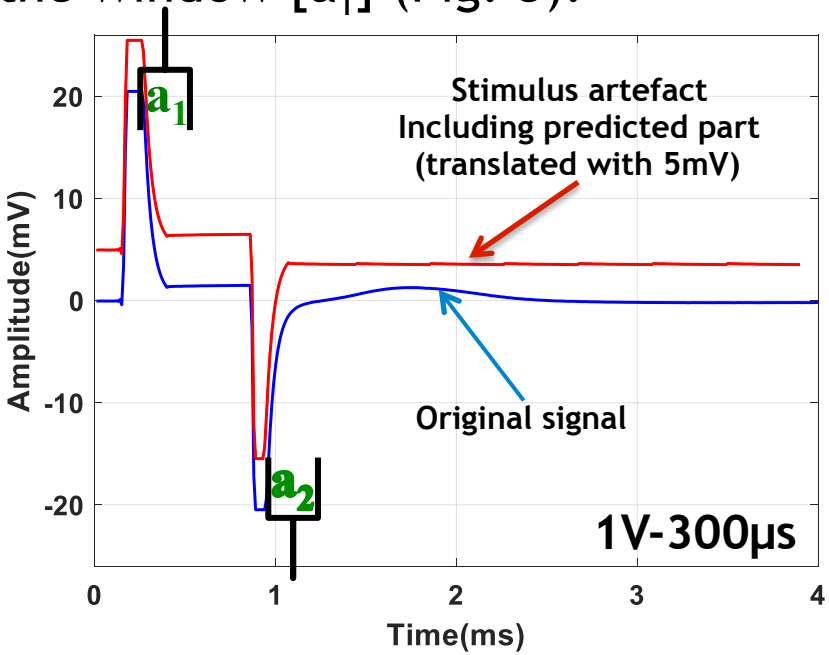


Fig.3 Example of truncated signal

- Hypothesis validation and reconstruction quality was assessed with Normalized Mean Square Error (NRMSE).

# Numerical results

## ❑ Stimulus artefact removal

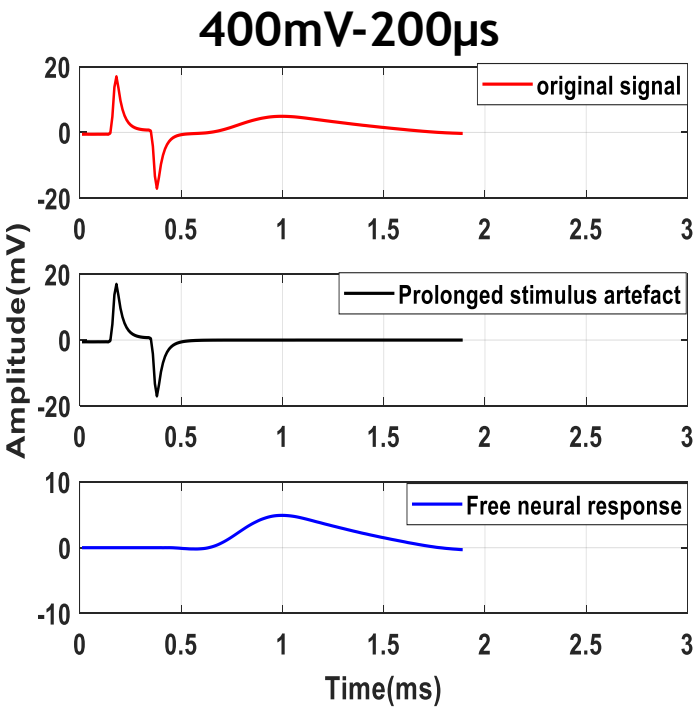


Fig.4 Example of stimulus artefact removal (response and artefact separated)

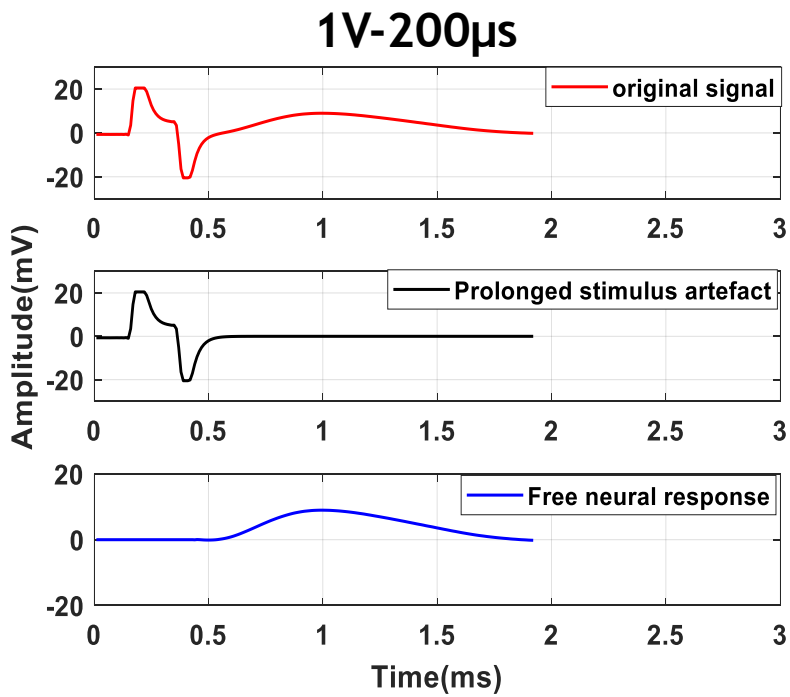


Fig.5 Example of stimulus artefact removal (case of saturation)

# Main results

- Existing hardware methods causes distortion of neural response in the case where stimulus artefact overlap neuronal response,
- Implemented method remove successfully stimulus artefact,
- Decomposing stimulus artefact into two symmetrical part is very useful in stimulus artefact identification and suppression,
- Unlike existing software method (based on template substraction) the stimulus artefact is directly identified from the processed data which reduce residual signals after its removal,
- In the case of stimulus artefact saturation, symmetry is not respected; predicting the artefact evolution from early samples gave promising results,
- Predicting contaminated part of stimulus artefact using matrix pencil method can be a solution.

# Recording nervous activity of a rat

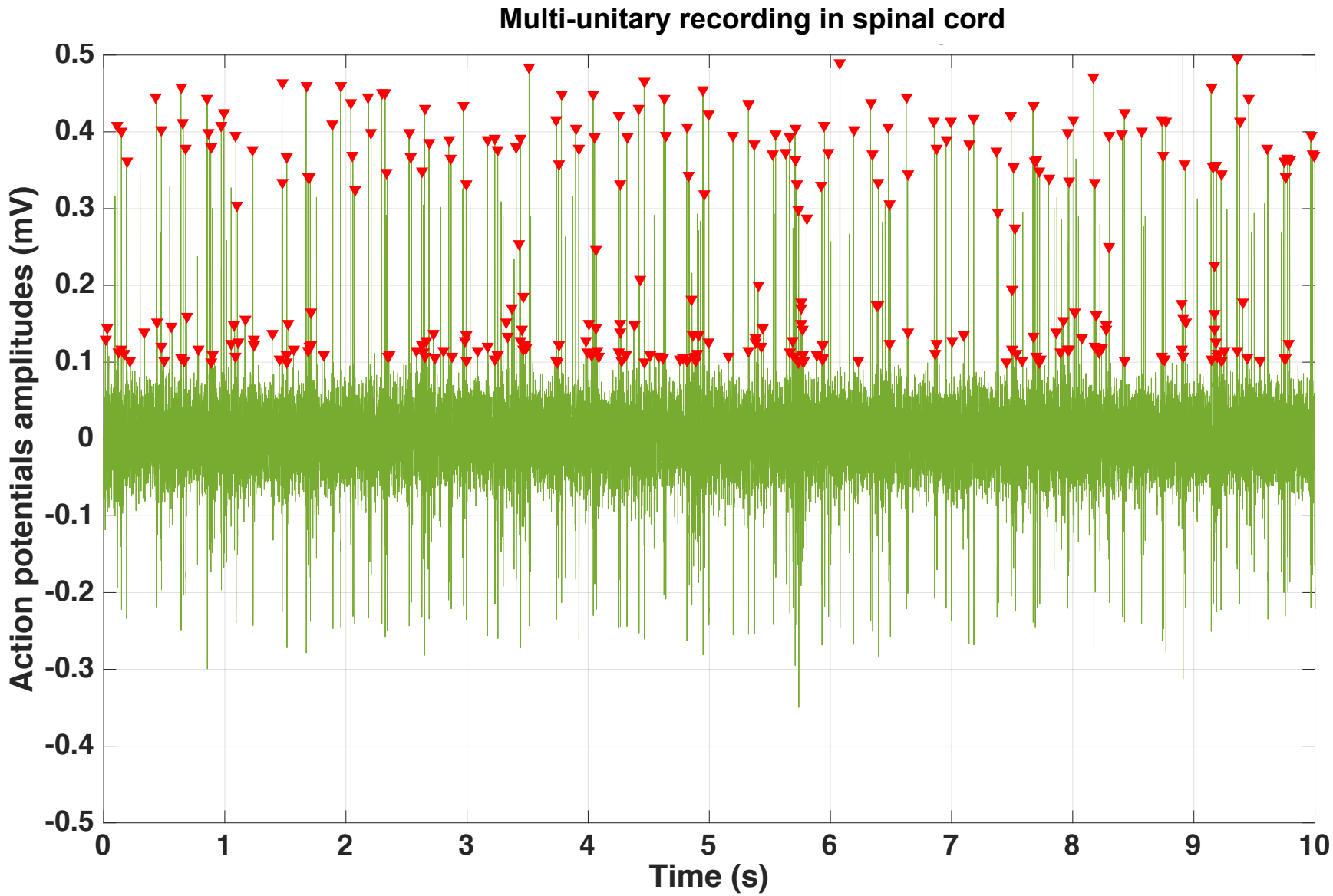

# Extraction of action potentials

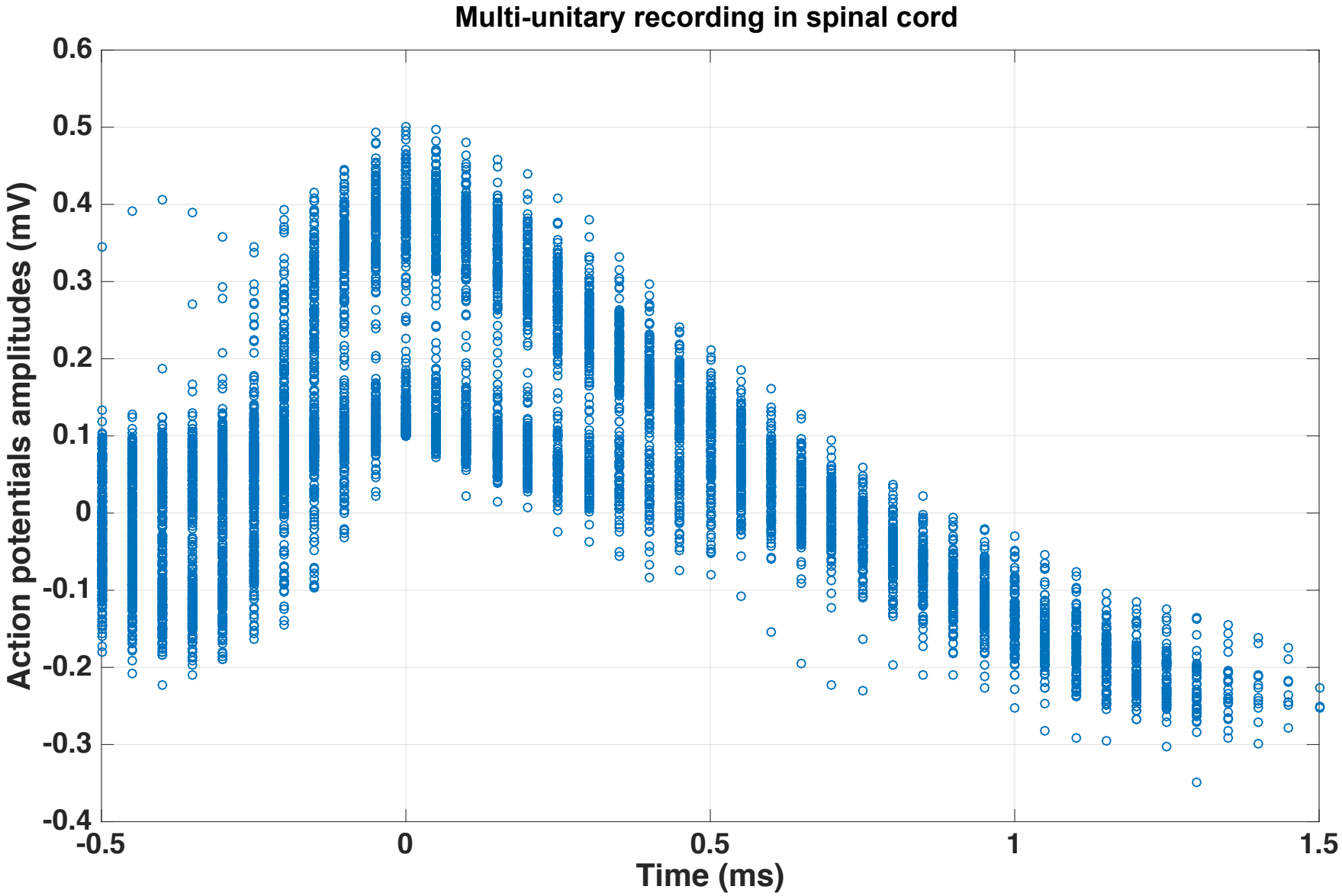

# Matrix Pencil method identification

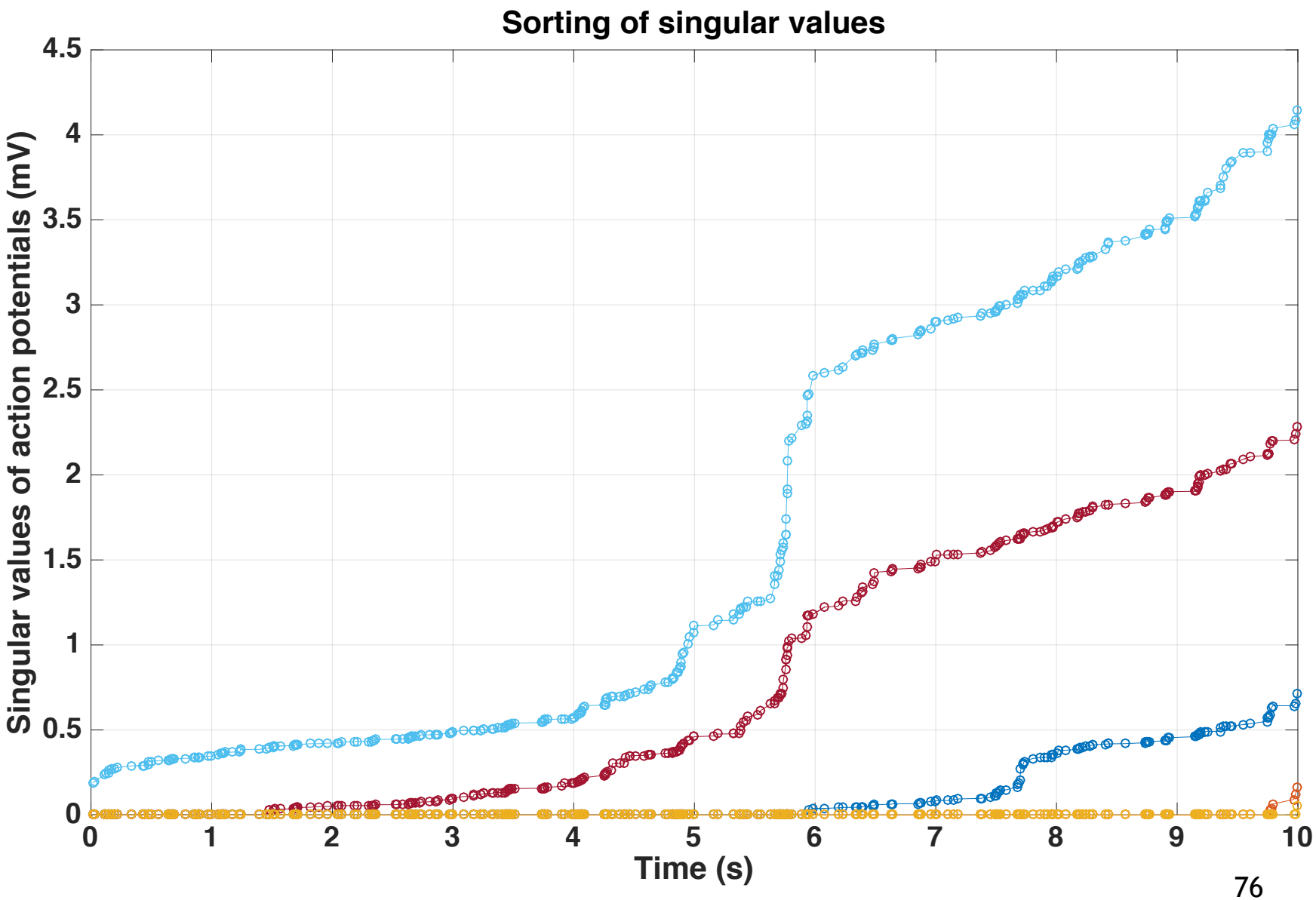

# Classification of action potentials

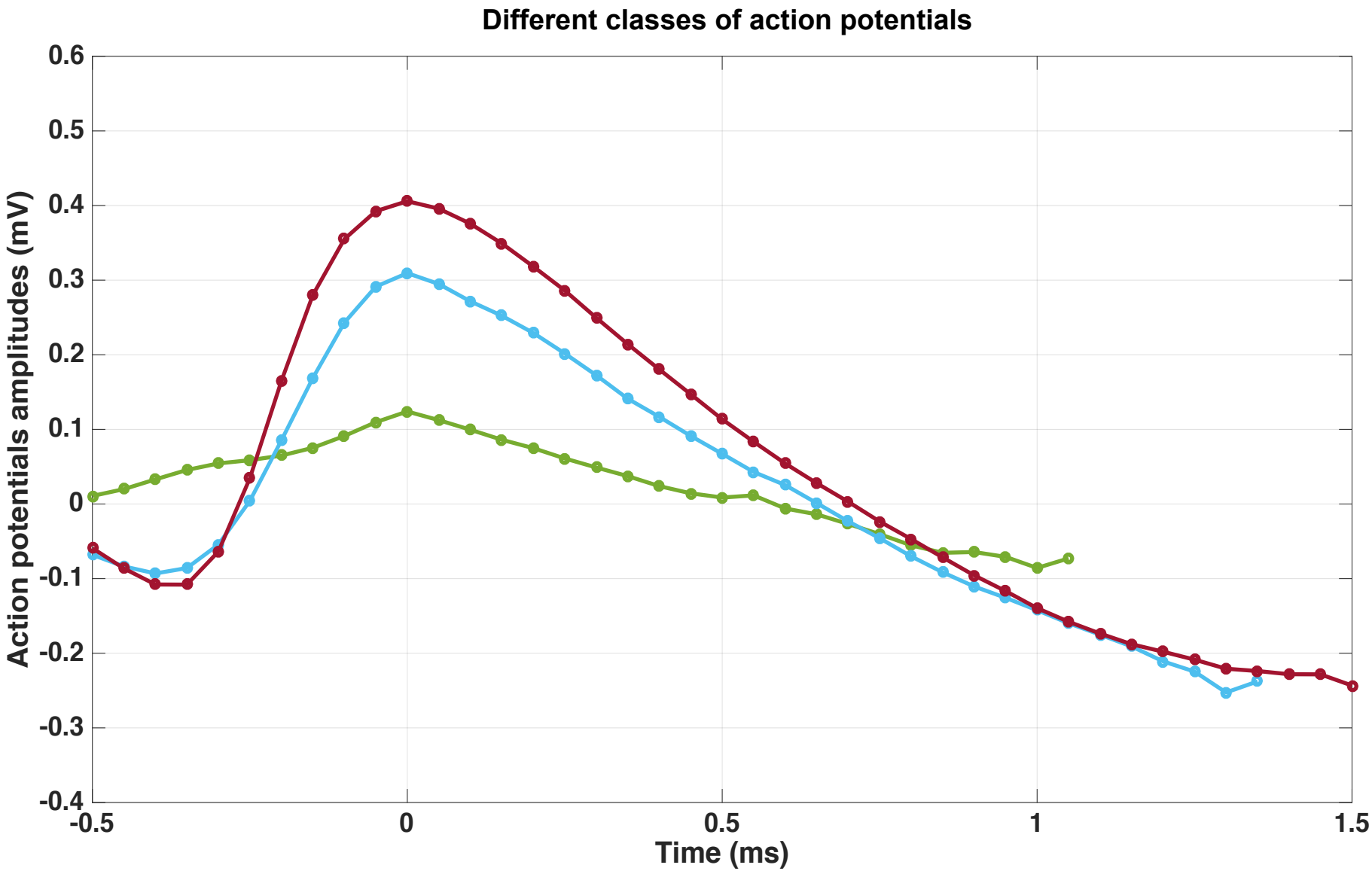

# Results

- Existing hardware methods causes distortion of neural response on the case where stimulus artefact overlap neural response,
- Implemented method remove successfully stimulus artefact,
- Decomposing stimulus artefact into two symmetrical part is very useful in stimulus artefact identification and suppression,
- Unlike existing software method (based on template substruction) the stimulus artefact is directly identified from the processed data which reduce residues after its removal,
- In the case of stimulus artefact saturation, symmetry is not respected; prolonging the artefact from early samples gave promising results,
- Predicting contaminated part of stimulus artefact using matrix pencil method can be a solution.

# Summary

- In this work, we present our contribution to analyze Electrophysiological Activities (ENG).
- The Matrix Pencil Method shows several advantages:
  - Robustness against measurement noises,
  - Predicting contaminated part of stimulus artefact,
  - Less data required to identify the original signal by using reduced number of poles and residues.
- Classification of action or field potentials.
- Expectation to extract nociceptive signal fibers Aδ and C.
- Extension to EEG diagrams.
- Correlation to Migraine patients.

# Applications of Matrix Pencil Method

## Evaluation of the Radiation from thin wire systems

- Identification of the current distribution (**space domain**).
- **Objective:** To evaluate the radiated EM field by using current and derivatives at geometric and electric discontinuities.

## Target Classification by using UWB radar

- Classification of fixed and moving targets under smart mobility (**frequency domain**).
- **Objective:** Complete the visual sensors (on board cameras) with Ultra Large Band Radar to classify obstacles more sufficiently.

## Non Intrusive Load Monitoring Appliance

- Smart Metering : Identification of electric loads by using the load curve already existed at the power meter (**time domain**)
- **Objective:** Electric billing detail including relevant uses (lighting, heating and domestic hot water)

# Applications of Matrix Pencil Method

## ❑ Analysis of Electro-physiological activities by Matrix Pencil Method

- Classification of action or field potentials (**time domain**).
- **Objective:** Have a better understanding of **pain message** and **its propagation** from the peripheral to the central nervous system.

# Thank you for your attention!

# Any questions?

# Appendices

# Electromagnetic field in cylindrical coordinates

Avec : $G_{-1} = \int R_0 \, G_0 \, dR_0$

$$G'_0 = \frac{\partial G0}{\partial R0}$$

$$G'_{-1} = \frac{\partial G-1}{\partial R0}$$

$$G''_{-1} = \frac{\partial^2 G-1}{\partial R0^2}$$

$$I' = \frac{\partial I}{\partial Z0}$$

$$I'' = \frac{\partial^2 I}{\partial Z0^2}$$

# Vector Potential

## In the case of integral part included

$$\vec{A} = \frac{\mu}{4\pi}\int I(Z)\,G(Z)\,dZ\vec{e_z}$$

Green function for homogeneous media

$$I(Z_0) = \sum_{h=1}^{M} R_h\ e^{S_h Z_0}$$

Mathematical Model

Electromagnetic Fields

The vector potential is expressed as the finite sum of M elementary potential vectors

$$\vec{A} = \frac{\mu}{4\pi}\sum_{h=1}^{M} R_h \int_0^L e^{S_h Z_0} G_0\ dZ_0\vec{e_z}$$

$$\vec{A_h} = \frac{\mu}{4\pi} R_h \int_0^L e^{S_h Z_0} G_0\ dZ_0\vec{e_z}$$

$$\vec{A} = \sum_{h=1}^{M} \vec{A_h}$$

# Radiation from thin wire systems

- Electromagnetic Fields series expressions:

$$\vec{H}_\phi = -\frac{1}{4\pi}\sum_{h=1}^{M} R_h \int_0^L e^{S_h Z_0} \sin\theta_0 \frac{\partial G_0}{\partial R_0} dZ_0 \vec{e_\phi}$$

$$\vec{E}_\rho = \frac{\eta}{4\pi\gamma}\sum_{h=1}^{M} R_h \left( S_h \int_0^L e^{S_h Z_0} \sin\theta_0 \frac{\partial G_0}{\partial R_0} dZ_0 - \left[ e^{S_h Z_0} \sin\theta_0 \frac{\partial G_0}{\partial R_0} \right]_0^L \right) \vec{e_\rho}$$

$$\vec{E}_z = \frac{\eta}{4\pi\gamma}\sum_{h=1}^{M} R_h \left( \begin{array}{c} (S_h^2 - \gamma^2) \int_0^L e^{S_h Z_0} G_0 dZ_0 \\ - \left[ e^{S_h Z_0} \left( \cos\theta_0 \frac{\partial G_0}{\partial R_0} + S_h G_0 \right) \right]_0^L \end{array} \right) \vec{e_z}$$

- It is important to stress out that these expressions are general.
- They are problem dependent - in order to choose the corresponding Green function.